



André Filipe Robalo de Oliveira

Graduated in Biochemistry

**Development of Chitin-Glucan Polymeric Structures Using
Biocompatible Ionic Liquids**

Dissertation for obtaining the Master degree in Biotechnology

Advisor: Doctor Luísa Alexandra Graça Neves,
Assistant Researcher, FCT-UNL

Jury:

President: Prof. Dr. Pedro Miguel Calado Simões

Arguer: Dr. Joana Oliveira Pais

Vowel: Dr. Luísa Alexandra Graça Neves



**FACULDADE DE
CIÊNCIAS E TECNOLOGIA
UNIVERSIDADE NOVA DE LISBOA**

September 2016

André Filipe Robalo de Oliveira

Graduated in Biochemistry

Development of Chitin-Glucan Polymeric Structures for Using Biocompatible Ionic Liquids

Dissertation for obtaining the Master degree in Biotechnology

Advisor: Doctor Luísa Alexandra Graça Neves,

Assistant Researcher, FCT-UNL

September 2016

Development of Chitin-Glucan Polymeric Structures Using Biocompatible Ionic Liquids

“Copyright” André Filipe Robalo de Oliveira, FCT/UNL e UNL

A Faculdade de Ciências e Tecnologia e a Universidade Nova de Lisboa têm o direito, perpétuo e sem limites geográficos, de arquivar e publicar esta dissertação através de exemplares impressos reproduzidos em papel ou de forma digital, ou por qualquer outro meio conhecido ou que venha a ser inventado, e de a divulgar através de repositórios científicos e de admitir a sua cópia e distribuição com objectivos educacionais ou de investigação, não comerciais, desde que seja dado crédito ao autor e editor.

“Our deepest fear is not that we are inadequate. Our deepest fear is that we are powerful beyond measure. It is our light not our darkness that most frightens us. We ask ourselves, Who am I to be brilliant, gorgeous, talented, fabulous? Actually, who are you *not* to be? You are a child of God. Your playing small does not serve the world. There is nothing enlightened about shrinking so that other people won’t feel insecure around you. We are all meant to shine, as children do. We were born to make manifest the glory of God that is within us. It’s not just in some of us; it’s in everyone. And as we let our own light shine, we unconsciously give other people permission to do the same. As we liberated from our own fear, our presence automatically liberates others.”

Marianne Williamson, *A Return To Love: Reflections on the Principles of A Course in Miracles*, 1992

Acknowledgments

Após vários anos nesta bela casa, Faculdade de Ciências e Tecnologia da Universidade Nova de Lisboa, gostaria de deixar o meu agradecimento às pessoas que contribuíram para o final desta minha última etapa a nível académico.

À minha orientadora, Dr.^a Luísa Neves, por me ter aceite como seu orientando. Foi um prazer poder trabalhar com uma pessoa que transpira boa disposição e simpatia. Muito obrigado por toda ajuda, disponibilidade e paciência para todos os meus obstáculos ao longo deste percurso, assim como por ter sido uma grande amiga durante este tempo todo.

Ao Professor Vítor Alves do Instituto Superior de Agronomia, por toda a calma e paciência na explicação de novas técnicas aprendidas, assim como toda a sua disponibilidade para ajudar no que sempre precisei para os resultados efectuados no seu laboratório.

Ao Nuno Costa e à Carla Rodrigues, pelo seu trabalho na análise de HPLC e TGA, simpatia perante os meus e-mails de esclarecimento de dúvidas ou quando tocava à porta do seu laboratório, tal como todo o esforço na entrega dos resultados obtidos, apesar de todas as dificuldades que foram impostas durante o processo.

Ao grupo BIOENG, nomeadamente à Dr.^a Filomena Freitas e à Inês Farinha, por todo o acompanhamento na fase de produção, preocupação, ajuda e auxílio que me disponibilizaram nesta etapa da tese.

Ao grupo LMP, nomeadamente às minhas colegas de laboratório, por toda a simpatia, amizade e boa disposição que demonstraram ao longo de todo este tempo, e, ainda, por me terem facilitado a tarefa de ter sido, durante a maior parte do tempo, o único “homem” no laboratório.

Aos meus colegas de Tese de Mestrado, Sofia Pereira, Patrícia Reis, Liliana Beatriz, João Ricardo e José Malta, pela companhia à hora de almoço, gargalhadas e brincadeira. Sem a vossa companhia nalgumas fases da tese, teria sido muito mais complicado para eu estar sozinho.

Aos meus grandes amigos do andebol e Salvaterra, um muito obrigado pelas horas que passámos juntos, que serviram para por os problemas de parte e aproveitar a companhia dos amigos.

À Catarina e ao Filipe, pela amizade ao longo dos anos, e principalmente nestas etapas mais importantes nas nossas vidas. São um orgulho para mim. Obrigado por poder contar sempre convosco e por terem a vossa casa sempre à minha disposição!

À Carolina, minha namorada e companheira de dramas e desilusões na tese, obrigado por todas as palavras de conforto que me dirigiste nas alturas em que mais precisei de apoio, assim como toda a confiança que sempre depositaste em mim! Dizer só “obrigado” não chega.

Por fim, um agradecimento especial para quem me tornou na pessoa que sou hoje. Aos meus pais e ao meu irmão, por todo o apoio que me deram ao longo da minha caminhada de formação pessoal e profissional.

A todos vós, dedico este trabalho.

Resumo

O objectivo desta dissertação de mestrado foi a produção e caracterização de estruturas poliméricas obtidas pela dissolução do complexo de quitina-glucanos, um co-polímero presente na parede celular de fungos e leveduras, através de quatro líquidos iónicos biocompatíveis à base da colina, onde foi variada a sua cadeia alquilo. Os líquidos iónicos seleccionados para este estudo apresentaram um comportamento típico de um fluido Newtoniano, onde foram caracterizados tendo em conta a sua quantidade em água, densidade e viscosidade.

Foram comparados dois complexos de quitina-glucanos de origens diferentes. Foi utilizado um produto comercializado pela empresa Kitozyme, o KiOsnutrime-CG, produzido pelo fungo *Aspergillus niger*. Por outro lado, foi produzido num laboratório pertencente ao grupo de investigação BIOENG, um complexo de quitina-glucano, extraído da parede celular da levedura *Komagataella pastoris*. Ambos os polímeros foram caracterizados consoante a sua composição em açúcares e propriedades térmicas.

Após a dissolução destes polímeros nos diferentes líquidos iónicos, as misturas foram submetidas ao método de inversão de fase, que visa retirar a quantidade de líquido iónico presente na estrutura polimérica. Deste modo, foram obtidos filmes à base do polímero comercial e laboratorial, e ainda um gel à base do polímero laboratorial. Os filmes foram caracterizados tendo em conta o seu conteúdo em açúcares, propriedades térmicas, morfologia por SEM, ângulos de contacto, swelling, permeabilidade aos gases, propriedades mecânicas e de adesividade. O hidrogel produzido foi colocado em ambientes a diferentes actividades de água, onde seguiu uma caracterização face ao seu conteúdo em açúcares, propriedades térmicas, morfologia por SEM, propriedades reológicas e de adesividade.

Palavras-Chave

Biopolímero; Complexo Quitina-Glucano; Líquido Iónico; Biocompatível; Revestimento para feridas

Abstract

The objective for this master thesis was the production and characterization of polymeric structures obtained by dissolving the chitin-glucan complex, a co-polymer present in the cell walls of fungi and yeasts, through four biocompatible choline based ionic liquids, where it was varied the alkyl chain. The ionic liquids selected for this study showed a typical Newtonian fluid behavior, which were characterized with regard to their water content, density and viscosity.

Two chitin-glucan complex from different sources were compared. A commercial product by Kitozyme company was used, KiOnutrime-CG, produced by the fungus *Aspergillus niger*. On the other hand, it was produced in a research group, BIOENG, a chitin-glucan complex extracted from the yeast cell wall, *Komagataella pastoris*. Both polymers were characterized according to its sugar composition and thermal properties.

After dissolution of these polymers in various ionic liquids, the mixtures were subdued to the phase inversion method, which aims to remove the amount of ionic liquid present in the polymeric structure. Thus, films were obtained from both commercial and laboratorial polymer, and also a gel based in laboratorial polymer. The films were characterized with regard to its sugar composition, thermal properties, morphology by SEM, contact angles, swelling, gas permeability, mechanical and adhesiveness properties. The hydrogel produced was place in environments at different water activities, which followed a characterization relative to their sugar content, thermal properties, morphology by SEM, rheological and adhesiveness properties.

Keywords

Biopolymer; Chitin-Glucan Complex; Ionic Liquids; Biocompatible; Wound dressing

List of Contents

Acknowledgments	ix
Resumo	xi
Abstract	xiii
List of Contents	xv
List of Figures	xix
List of Tables	xxi
Abbreviations	xxiii
1. Introduction	1
1.1 Biopolymers and its Applications	1
1.2 Chitin and Chitosan	1
1.3 Glucan	2
1.4 Chitin-Glucan Complex Characteristics	3
1.5 Ionic Liquids	4
1.6 Wound Dressing Materials	5
1.7 Thesis Objective	6
2. Materials and Methods	7
2.1 Ionic Liquids	7
2.1.1 Ionic Liquids Characterization	7
2.1.1.1 Water Content	7
2.1.1.2 Density	8
2.1.1.3 Viscosity Measurements	8
2.1.1.4 Thermal Properties	8
2.2 Chitin-Glucan Complex Biopolymers	9
2.2.1 Chitin-Glucan Complex Production and Extraction	9
2.3 Chitin-Glucan Complex Polymers Characterization	10
2.3.1 Chitin-Glucan Complex Sugar Composition	10
2.3.2 Thermal Properties	11
2.4 Films and Hydrogels Preparations	11
2.5 Chitin-Glucan Complex Mixtures Characterization	11

2.5.1	Chitin-Glucan Complex Mixtures Sugar Composition	12
2.6	<i>Chitin-Glucan Complex Films Characterization</i>	12
2.6.1	Films Sugar Composition	12
2.6.2	Thermal Properties	12
2.6.3	SEM Analysis.....	12
2.6.4	Contact Angle Measurements.....	13
2.6.5	Swelling Tests	13
2.6.6	Permeability Tests	13
2.6.7	Mechanical Properties	14
2.6.8	Adhesion Test.....	16
2.7	<i>CGC Hydrogels Characterization</i>	16
2.7.1	Hydrogels Sugar Composition	16
2.7.2	Thermal Properties	16
2.7.3	SEM Analysis.....	17
2.7.4	Rheology Tests.....	17
2.7.5	Adhesion Test.....	17
3.	Results and Discussion	19
3.1	<i>Ionic Liquids Characterization</i>	19
3.1.1	Ionic Liquids Water Content and Density	19
3.1.2	Viscosity Measurements.....	20
3.2	<i>Chitin-Glucan Complex Sugar Composition</i>	21
3.3	<i>Chitin-Glucan Complex Thermal Properties</i>	24
3.4	<i>Chitin-Glucan Complex Films Characterization</i>	24
3.4.1	SEM Analysis.....	24
3.4.2	Contact Angle Analysis.....	26
3.4.3	Swelling Tests	27
3.4.4	Permeability Tests	28
3.4.5	Mechanical Properties	29
3.4.6	Adhesion Measurements	30
3.5	<i>CGC Hydrogels Characterization</i>	31
3.5.1	SEM Analysis.....	31

3.5.2	Rheology Tests	33
3.5.2.1	Dynamic State Measurements	33
3.5.3	Adhesion Measurements	34
4.	Conclusion.....	37
5.	Future Work	39
6.	References	41
7.	Appendices	45

List of Figures

Figure 1.1 - Molecular structure and hydrogen bond in (a) α -chitin and (b) β -chitin [6].....	2
Figure 1.2 - Schematic structure of chitin and chitosan [4].....	2
Figure 1.3 - Possible applications of Ionic Liquids [25].	4
Figure 2.1 – Scheme of experimental set-up for measuring the pure gas permeability of the CGC films, where TC is Temperature Controller and PI is Pressure Indicator [39].	14
Figure 2.2 - Puncture test scheme.	15
Figure 2.3 – <i>In Vitro</i> bonding strength measurement scheme, where the pork skin is represented by the pink square and the samples are represented by the yellow form. The direction of the force applied in the samples is demonstrated by the arrow.	16
Figure 3.1 - SEM images of top surface and cross-section of CGC-Com films. Images amplification for top surface and cross-section are, respectively: Choline Acetate CGC-Com – x1000 and x75; Choline Propionate CGC-Com – x500 and x100; Choline Isobutanoate CGC-Com – x500 and x500; Choline Hexanoate CGC-Com – x500 and x200.	25
Figure 3.2 - SEM images of top surface and cross-section of CGC-FCT films. Images amplification for top surface and cross-section are, respectively: Choline Acetate CGC-FCT – x2000 and x35; Choline Propionate CGC-FCT – x1000 and x100; Choline Hexanoate CGC-FCT – x1000.	26
Figure 3.3 - Contact angle of CGC-Com films produced by different ionic liquids.	27
Figure 3.4 – SEM images of top surface of choline isobutanoate CGC-FCT hydrogels. Images amplification for top surface are: Hydrogel with $a_w = 0.216$ – x1000; Hydrogel with $a_w = 0.514$ – x1000; Hydrogel with $a_w = 0.751$ – x1000; Hydrogel with $a_w = 0.923$ – x1000.	32
Figure 3.5 - Frequency sweeps for CGC hydrogels, (a) H1 – hydrogel with $a_w = 0.216$, (b) H2 – hydrogel with $a_w = 0.514$, (c) H3 – hydrogel with $a_w = 0.751$ and (d) H4 – hydrogel with $a_w = 0.923$	34
Figure 7.1 – Glucose calibration curve.	45
Figure 7.2 - Mannose calibration curves.	45
Figure 7.3 - Glucosamine calibration curve.	46
Figure 7.4 - Tension in function of the shear rate at different temperatures, 30°C, 80°C and 110°C, for choline acetate ionic liquid.	47
Figure 7.5 - Tension in function of the shear rate at different temperatures, 30°C, 80°C and 110°C, for choline propionate ionic liquid.	47
Figure 7.6 - Tension in function of the shear rate at different temperatures, 30°C, 80°C and 110°C, for choline isobutanoate ionic liquid.	48
Figure 7.7 - Tension in function of the shear rate at different temperatures, 30°C, 80°C and 110°C, for choline hexanoate ionic liquid.	48
Figure 7.8 - Representation choline acetate viscosity as a function of temperature.	49
Figure 7.9 - Representation choline propionate viscosity as a function of temperature.	49

Figure 7.10 - Representation choline isobutanoate viscosity as a function of temperature.	50
Figure 7.11 - Representation choline hexanoate viscosity as a function of temperature.	50
Figure 7.12 - Deformation curves of choline acetate CGC-Com.	51
Figure 7.13 - Deformation curve of choline propionate CGC-Com.	51
Figure 7.14 - Deformation curves of choline isobutanoate CGC-Com.	52
Figure 7.15 - Deformation curves of choline hexanoate CGC-Com.	52

List of Tables

Table 2.1 – Molecular formula and molecular weight of cholinium-based ionic liquids used.	7
Table 2.2 - Different water activities used at the desiccators [38].	11
Table 3.1 - Water content and density of the cholinium based ionic liquids.....	19
Table 3.2 - Viscosity and activation energy of the ionic liquids used.....	20
Table 3.3 – Sugar constituents in CGC polymers and polymeric materials.	23
Table 3.4 – Swelling results of CGC films.....	28
Table 3.5 - CPC and CHC permeability values for N ₂ , O ₂ and CO ₂ gases and selectivity values of CO ₂ /N ₂ , CO ₂ /O ₂ and N ₂ /O ₂	29
Table 3.6 – Mechanical properties of commercial CGC films, where τ_p is the puncture stress and ε the puncture elongation.	29
Table 3.7 - Maximum tension values of CGC laboratory films for adhesion measurements.	30
Table 3.8 - Maximum tension values of CGC laboratory hydrogels for adhesion measurements.	34

Abbreviations

a_w – Water activity

CGC – Chitin-Glucan Complex

CGC-Com – Commercial Chitin-Glucan Complex

CGC-FCT – Chitin-Glucan Complex produced in laboratory

HCl – Hydrochloric Acid

ILs – Ionic Liquids

Rpm – Rotation per minute

SEM – Scanning Electron Microscope

SLPM – Standard Liters per Minute

TFA – Trifluoroacetic Acid

v/ v – Volume per volume

1. Introduction

1.1 Biopolymers and its Applications

Biotechnological advancements allowed the use of new resources, more economical and efficient, for diverse areas. The interest for biopolymers increased, once it is possible not only to be independent of fossil fuels, but also these macromolecules show properties that can be useful into a variety of applications in different areas, such as cosmetic, biomedical and food packaging [1-2].

Given the high interest on the use of natural polymers in many fields of medicine, in this master thesis, a microbial biopolymer, Chitin-Glucan Complex, will be used to prepare polymeric structures, gels and films, and their potential for wound treatment applications will be evaluated.

1.2 Chitin and Chitosan

After cellulose, chitin is the most abundant polysaccharide, which can be found in the exoskeleton of arthropods, and in the cell wall of fungi and yeasts. It has been reported as a possible promise for applications in biomedicine field, such as for wound dressing, reports stated that wound dressing materials based on chitin can accelerate the repair of the tissue and regulate the secretion of inflammatory mediators, or in tissue engineering, because chitin has ideal properties of degradability, immunogenicity and mechanical strength, to act as a scaffold [3-4].

Chitin is a linear homo-polymer composed by a 1→4 linkage of N-acetyl-D-glucosamine [4]. This polymer has 3 different polymorphic forms: α , β and γ , which the last one is just a variant of the α -form [5]. The other forms vary in terms of packing the adjacent chain and their polarity [6]. In both structures, these chains are organized in sheets, with several intra-molecular hydrogen bonds [7]. The hydrogen bond between C-O-NH lead into an intra-crystalline structure of both α - and β -form. This last one is stronger, which can provide a more parallel arrangement in the structure as demonstrated on Figure 1.1 [8].

A study of Saito *et al* demonstrated that, when β -chitin is supplemented with an aqueous solution of HCl 7 M and concentrations above, a total rupture occurs between the intermolecular hydrogen bonds, leading to a loss of the crystalline structure of this form. It was also observed that when it is washed using water, structures of chitin can be obtained in the α -form, which points to the conclusion that is possible to convert the β -form into the α -form [9]. Besides that, if chitin is put under some alkaline conditions, such as concentrated sodium or potassium hydroxide solution at 100°C or higher, it suffers a partial deacetylation. According to the chitin's source, his degree of deacetylation can vary. Once the deacetylation is about 50% the polymer results on its most important derivative,

chitosan [8, 10]. By this fact, the derivative of chitin is composed by linear 1→4 N-acetyl-D-glucosamine and glucosamine residues [4].

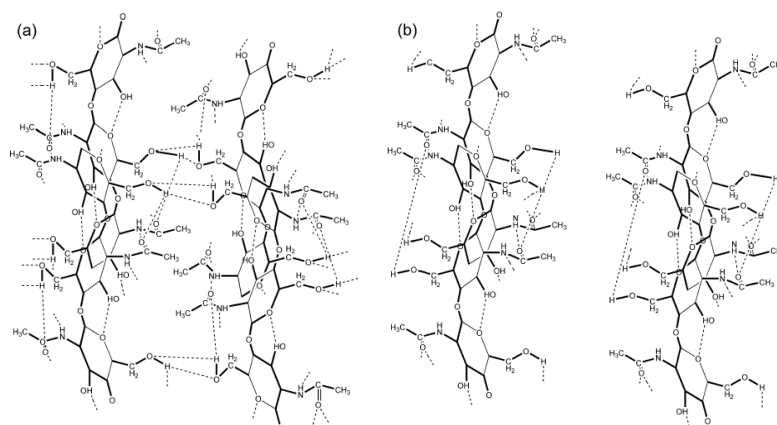


Figure 1.1 - Molecular structure and hydrogen bond in (a) α -chitin and (b) β -chitin [6].

Chitin and chitosan are polymers that share the same macromolecular identity, but differ in the acetylation fraction of the repeating units (Figure 1.2) and, by that, share the same properties. They are non-toxic, have physiological inertness, antibacterial properties, gel-forming properties, biocompatibility and biodegradability [8].

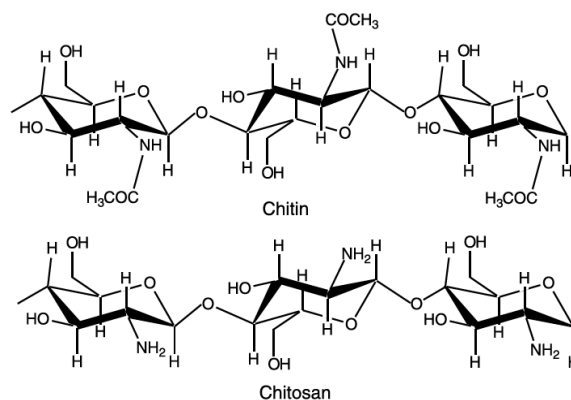


Figure 1.2 - Schematic structure of chitin and chitosan [4].

1.3 Glucan

A biopolymer with a great promise in the field of biomedicine is the β -glucan, a polysaccharide comprised of β -linked-D-glucose molecules, which can be found in plants, fungi or yeast cells. It is known that the properties of this polymer can vary, according to their structure, length of macromolecular and three-dimensional organization of the chains [11-12].

Several studies have described that β -glucan exhibit antitumor activity and may reduce inflammatory responses. It is also reported that is able to active macrophages and natural killer cells in order to reduce the quantity of tumor cells, as well as to induce and accelerate the production of cytokines, like TNF- α , IL-6 and IL-12. This happens due to its role as a biological response marker for the immune system [11, 13-14].

1.4 Chitin-Glucan Complex Characteristics

The Chitin-Glucan Complex (CGC) used in this master thesis, is a co-polymer composed by two types of polysaccharides, chitin, which has units of N-acetyl-D-glucosamine, and β -(1,3)-glucan, which has glucose units, covalently linked between them. This biopolymer can be found in the exoskeleton of shrimps and in the cell walls of fungus or yeasts [15].

In this work, two different CGC biopolymers produced by different sources, one by a fungus *Aspergillus niger* and other by the yeast *Komagataella pastoris*, will be studied.

One of the most global non-animal chitosan and chitin-glucan manufacturer, KitoZyme, uses the fungi *A. niger*, in order to produce the chitin-glucan compound. The strain of this microorganism does not have any genetically modification and is used in the food and pharmaceutical industries for the production of citric acid [16].

Another very commonly yeast specimen used in the pharmaceutical field for the production of heterologous proteins is *K. pastoris*, since the techniques utilized for its manipulation are especially easy [17]. This yeast possesses the advantage of using diverse and economical substrates, such as glycerol or methanol, for its growth and biomass production. *Komagataella pastoris* DSM 70877 yeast cell wall has in its composition the copolymer CGC, which confers integrity to the cell structure [18].

This co-polymer exhibits biocompatibility and biodegradability, accelerates wound healing and has antibacterial and anti-inflammatory properties [8]. By that, CGC has a wide range of potential applications in diverse areas, such as agriculture, food or biomedicine industries. The biomedical field is the one that CGC has a stronger promise, where can be used in tissue engineering, as a safe vehicle for drug delivery, or as wound dressing [19-20].

However, there is a major problem that lays in risk the utilization of this complex for biomedical applications. CGC is very difficult to process, once it is insoluble in water and in the most common organic solvents [21]. Though it is possible to solubilize chitin with strong acids, such as dichloroacetic acid and trichloroacetic acid, or with fluorinated solvents, like hexafluoroisopropyl alcohol, these kinds of solvents are unappealing for application in wound treatment, due to their

corrosive and toxic nature [22-23]. Once this problem is overcome, it is expected that this biopolymer in the form of gels, films or fibers, can be suitable for biomedical applications [8].

1.5 Ionic Liquids

The insolubility of high-value biopolymers has limited their use in several applications. Even though their inherent biocompatibility and biodegradability, the promise and potential for the biomedicine field is not being truly applied [1].

In the last years, a new fascinating class of “eco-friendly” solvents has been developed, with particular and interesting properties, such as negligible vapour pressure and high thermal stability. This novel type of solvents is designated by ionic liquids (ILs) and has been exploited in order to replace the volatile organic compounds often used in several industrial applications. Possible applications of ionic liquids are depicted in Figure 1.3 [24-25].

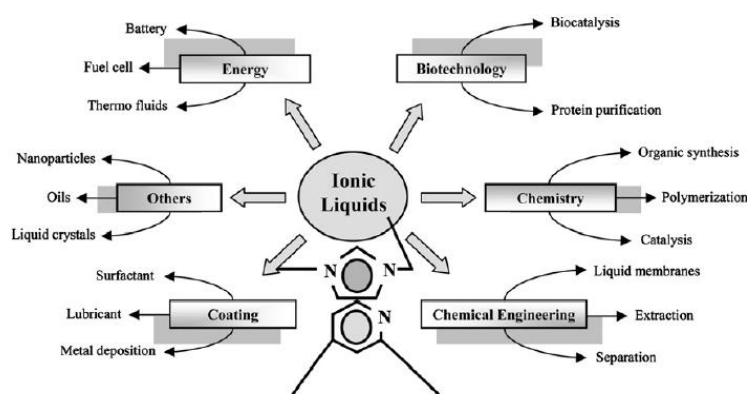


Figure 1.3 - Possible applications of Ionic Liquids [25].

Basically, an ionic liquid is composed by salts with melting point below 100°C. For this to happen, the solvent should have asymmetry of at least one of the ions and a low intermolecular attractions, beyond to the ionic attraction [26]. ILs can be obtained by a combination of large cations with several anions. This number of rearrangements between cations and anions are one of the advantages for the potential utilization of ILs, which can be designated as “designer solvents”. The physical and chemical properties of the ILs may be tuned according to the cation and anion in their structure [24]. Studies have reported that the cation is very important for the toxicity of the IL and they should have small side chains – to confer less impact on living cells – and preferentially an ester group to increase their biodegradability. On the other hand, the anion is important for the ILs properties, such as solubility and viscosity, and also contribute to the overall toxicity [27]. Once the toxicology of this kind of solvents is controlled and they show biocompatible behaviour, ILs can be

used for the dissolution of biopolymers, such as chitin-glucan complex, aiming their use in the biomedical field [1].

The quaternary ammonium cation, cholinium, $[\text{NMe}_3(\text{CH}_2\text{CH}_2\text{OH})]^+$, is an essential micronutrient for the functioning of the cells and cholinium-based ILs have been reported as being biodegradable and non-toxic [28]. Petkovic *et al* combined alkanoates with long side chains, with cholinium in order to evaluate the anion effect on the IL toxicity in filamentous fungi. The study reported that choline-based ionic liquids can be used in biotechnological applications, once they are environmentally benign and biocompatible and were less toxic than their corresponding sodium salt-based ionic liquids [29].

To dissolve biopolymers, a solvent must be capable to disrupt the hydrogen bonds present in their structure [30]. Mantz *et al* demonstrate that imidazolium chlorides ionic liquids are a viable solvent for the dissolution of some biopolymers, like cellulose, chitin and collagen [30]. Other studies have also reported that biopolymers can be dissolved in a variety of ionic liquids, which reveal that the ILs are a new generation of solvents capable to valorize the use of these macromolecules [1, 30].

Due to choline-based ILs biocompatible properties and their possible ability to disrupt strong hydrogen bonds of biopolymers, these solvents were selected for this master thesis.

1.6 Wound Dressing Materials

The wound treatment has been used since the ancient times, where the dressing material was applied to stop the bleed and protect the wound from external disturbances. Since the skin is the major organ of the human body it is crucial to protect when it is damaged, once it is very important for the homeostasis and the prevention of microorganisms' infections [4].

Jayakumar *et al* stated that the ideal dressing should be non-toxic, non-allergenic, nonadherent, easily removed and it should be made from an available biomaterial that requires minimal processing, with antimicrobial and wound healing properties. This type of biomaterial should maintain a moist environment at the wound surface, allow a gaseous exchange, act as a barrier to microorganisms and remove excess exudates [4].

Nowadays, there are three different types of wound dressings: biologic, synthetic and biologic-synthetic. The first can be composed by pigskin and is used very often clinically. It has some disadvantages, such as high antigenicity, poor adhesiveness and risk of contamination. Synthetic dressings can be applied at bending surfaces, like joints, and have long life, however has the disadvantage of accumulate the wound exudates, which could lead to a risk of pathogen infection.

Biologic-synthetic dressings are bilayered composed by polymeric and biologic materials, but it presents some disadvantages, like enable the proliferation of infections in some burn wounds [4, 31-32]. Commercially, there are wound dressing products based on chitin and chitosan and their derivatives. SyvekNT[®] is a patch composed by chitin isolated from *microalgae*, which promotes the rapid control of bleeding [34]. 3M[™] Tegaderm[™] +Pad is an adhesive, transparent film bonded to a low-adherent absorbent pad, indicated for surgical wound dressing and post-operative for patients released from hospital into the community, and Chitodine[®], a gel, good for wound disinfection and surgical healing, are both products based on chitosan and their derivatives [4,34].

The CGC present several biological properties, such as a natural adhesiveness and antimicrobial activity, which could be important for the treatment of skin wounds and also their regeneration. Biocompatibility property of CGC has been reported, which could indicate the promise of this biopolymer as a wound dressing material [36].

1.7 Thesis Objective

The main objective for this work is the development of polymeric materials based on CGC, namely films and hydrogels, using biocompatible choline-based ILs. This work is a continuation of some previous studies performed to the same biopolymer, where only choline acetate was tested [37].

The ionic liquids selected for this work were based on the cholinium cation and derived carboxylic acid anions, and were characterized in terms of water content, density and viscosity.

Two different CGC were tested, one biologically produced from FCT – Universidade Nova de Lisboa, and the other commercially available produced by Kitozyme. The polymers were characterized in terms of their sugar composition and thermal properties.

After the dissolution studies of the CGC biopolymers into the biocompatible ILs, water will be used as a non-solvent in phase inversion method to remove the IL from the polymeric structure. After this, different polymeric structure can be obtained, namely in the form of films and gels.

The polymeric film structure here prepared will be characterized regarding their sugar composition, thermal properties, morphology (by SEM), contact angle, swelling, gas permeability, mechanical and adhesion properties. In terms of the hydrogel produced, it will be characterized concerning their sugar composition, thermal properties, morphology, rheology behavior and adhesion properties.

2. Materials and Methods

2.1 Ionic Liquids

The ionic liquids used to dissolve the CGC were choline acetate, choline propionate, choline isobutanoate and choline hexanoate. These ILs were produced and provided by Professor Carlos Afonso, Faculdade de Farmácia, Universidade de Lisboa.

The molecular formula and molecular weight of these solvents are shown in Table 2.1.

Table 2.1 – Molecular formula and molecular weight of cholinium-based ionic liquids used.

Ionic Liquids	Molecular Formula	Molecular Weight (g/ mol)
Choline Acetate	$C_7H_{17}NO_3$	163.21
Choline Propionate	$C_8H_{19}NO_3$	177.24
Choline Isobutanoate	$C_9H_{18}NO_3$	191.17
Choline Hexanoate	$C_{11}H_{25}NO_3$	219.32

2.1.1 Ionic Liquids Characterization

The ionic liquids used were characterized in terms of their water content, density, viscosity at different temperatures and thermal properties.

2.1.1.1 Water Content

The measurement of the water content of the ionic liquids was performed using a 831 KF Coulometer (Metrohm, Switzerland) equipment. The sample was collected in a gas-tight syringe without any air and measured in an analytical balance. Then the sample was injected, its weight was introduced into the equipment and the water content displayed.

2.1.1.2 Density

To know the density of the ionic liquids at 30°C, a pycnometer was used. The density of the ILs was determined by using an analytical balance (Kern, Germany) and comparing it with a reference fluid. In this case distilled water was used, for which the density at different temperatures is known.

The weight of the pycnometer with 5 mL capacity must be measured as well as its weight with distilled water (m_{H_2O}) and ionic liquid (m_{IL}). Once the volume is constant it is possible to obtain the unknown density through the equation:

$$\rho_{IL} = \frac{m_{IL}}{m_{H_2O}} \times \rho_{H_2O} \quad \text{Eq. 2.1}$$

Where ρ_{IL} and m_{IL} are the density (g/m^3) and mass (g) of the ionic liquid, respectively, and ρ_{H_2O} and m_{H_2O} are the density (g/m^3) and mass (g) of the distilled water, respectively.

2.1.1.3 Viscosity Measurements

Viscosity measurements were done at Instituto Superior de Agronomia, Universidade Técnica de Lisboa, under the supervision of Professor Vítor Alves. These measurements were performed in a controlled stress rheometer, Haake MarsTM II (Thermo Scientific, Germany), which has a Peltier liquid temperature control unit. The cone and plate used had a diameter of 3.5 cm and 2° angle, and the experiments were executed at different temperatures, 30°C, 80°C and 110°C. The first temperature was taking into account the density measurements, in section 2.1.1.2, and the other ones are relative to CGC polymer solubilization, as it will be further explained in section 2.4.

2.1.1.4 Thermal Properties

Thermogravimetric measurements were carried out with a Labsys evo TG-TGA/DSC (Setaram, France), under argon atmosphere (50 mL/min) and loading 20 mg of each material into a covered aluminium crucible. One heating cycle was performed, where a ramp of 1°C/min from 25°C and 50°C was used.

2.2 Chitin-Glucan Complex Biopolymers

In this work, two different CGC biopolymers were studied, namely, co-polymers extracted from the cell walls of the yeast *Komagataella pastoris* and of the fungus *Aspergillus niger*. *K. pastoris* CGC was produced at Biochemical Engineering Group (BIOENG), Faculdade de Ciências e Tecnologia, Universidade Nova de Lisboa, in collaboration with Dr. Filomena Freitas. The production of this biopolymer was only closely accompanied. On the other hand, Kitozyme (Belgium) under the trade name KiOnutrime-CGTM (Kitozyme, Belgium) was used for comparison with the CGC produced under laboratorial conditions. In order to differentiate the two polymers referred above, for the *K.pastoris* CGC and commercial Kitozyme CGC was applied a nomenclature of CGC-FCT and CGC-Com, respectively.

2.2.1 Chitin-Glucan Complex Production and Extraction

For the production of chitin-glucan complex, the inoculum was prepared by inoculating 2 mL of the cryopreserved *K.pastoris* culture into 400 mL basal salt medium (BSM – 10.7 mL H₃PO₄ 85% (v/v) (Scharlau, Spain), 0.48 g CaSO₄·2 H₂O (Acros Organics, Belgium), 7.28 g K₂SO₄ (Chem-Lab, Belgium), 5.96 g MgSO₄·7 H₂O (LabChem, Portugal), 1.65 g KOH (EKA Chemicals, Netherlands), 24 g Glycerol (biodiesel product – SGC Energia, Portugal), 0.3 mL Antifoam Y-30 Emulsion (Sigma Aldrich, USA)), in shake flasks. The inocula were incubated at 30°C, for 40 h at 200 rpm, in a orbital shaker (Excella E24, Incubar Shaker Series). Then, the 400 mL culture was used to inoculate a 10 L bioreactor (Biostat[®] B plus, Sartorius) with an initial volume of 8 L, giving a percentage of the inoculums of 5 % (v/v). This experiment occurred for 48 h, approximately, under a batch mode. The following parameters were controlled: temperature (30°C), pH (5.00 – controlled by the automatic addition of NH₄OH 25 % (v/v)) and aeration (8 SLPM).

To monitor the cellular growth, some samples were taken periodically and the optical density (VWR International, USA) was measured at 600 nm. Once registered the OD between 70-75, it means the culture reached the stationary phase of growth, then a broth volume of 1000 mL was removed from the bioreactor and 200 g of NaOH (EKA Chemicals, Netherlands) was added to it to give a concentration of approximately 1 M. Due to the viscosity of this solution, 200 mL of deionized water were further added to dilute the mixture, giving a final volume of 1200 mL. Then, it was placed in a stirring plate and kept at 65°C for 2 h, so the cells were lysed and its alkaline components were solubilized [18]. After that time, the broth was cooled to room temperature.

Afterwards, the suspension was centrifuged at 10375 g, 22°C, for 10 min. The supernatant was discarded once the polymer was in the pellet – due to its insolubility in alkaline medium – as long as

other cellular components. The pH of the suspension was measured and adjusted with H₂SO₄ 0.01 N (Fisher Scientific, UK), until the value of 6.80 was reached. Then, the insoluble material was successively washed with deionized water by resuspending the insoluble pellet in water and centrifuging, always in identical conditions. The pH value (pH 1100 L, VWR pHenomenalTM, Portugal) and conductivity (Lab 960, Schott Instruments, Germany) of this suspension were measured after each resuspension in deionized water, until final values of 6.90 and 236 μ S/ cm, respectively, were reached. The majority of the inorganic salts from the medium and the excess of NaOH and H₂SO₄ were removed through these centrifugation steps, which guaranteed high polymer purity.

The final step that CGC underwent, was the liofilization process (CoolSafeTM, Denmark), at nearly vacuum conditions and 117°C, for approximately 48 h. The polymer was obtained in a powder form, with a total mass of 18.88 g.

2.3 Chitin-Glucan Complex Polymers Characterization

CGC-FCT and CGC-Com were characterized in terms of sugars composition, namely glucose, mannose and glucosamine, and thermal properties.

2.3.1 Chitin-Glucan Complex Sugar Composition

To determine the sugar composition of both CGC polymers, two hydrolysis procedures were done to cleave the β -glucan and chitin moieties of the co-polymers. Trifluoroacetic acid (TFA – Sigma Aldrich, USA) was used to hydrolyze the glucan present in the polymer into its glucose monomers, while hydrochloric acid (HCl – Sigma Aldrich, USA) was used to hydrolyze chitin and obtain glucosamine residues [21].

For the first procedure, TFA hydrolysis, dried CGC samples of 5 mg were suspended in 5 mL of deionized water and 0.1 mL of TFA 99 % (v/v) was added. The hydrolysis was performed at 120°C for 2 h. On the second procedure, HCl hydrolysis, the samples of 5 mg were resuspended in 5 mL of HCl 5 N. The hydrolysis was performed at 120°C for 5 h. Both of these hydrolysates were used for the sugar quantification performed in a Dionex ICS-3000 Ion Chromatography (Thermo Scientific, USA) using a Aminotrap + Carbopac PA10 250 x 4 mm THERMO column and 18 mM NaOH eluent with a flow of 1 mL/min. The temperature used was 30°C. In addition, 1 g/L glucose (Sigma-Aldrich, USA), 1 g/L mannose (Sigma Aldrich, USA) and 1 g/L glucosamine (Sigma Aldrich, USA) were used as standards and were treated by the same procedure as the polymer samples. The calibration curves are in Appendix I.

2.3.2 Thermal Properties

Same procedure described at 2.1.1.4 was done to the characterization of the two CGC polymers used.

2.4 Films and Hydrogels Preparations

In order to dissolve the CGC polymers, 5 wt. % of the biopolymers was added to the ionic liquid in a breaker glass. Then it was placed in a thermostat oil bath under continuous agitation, using a magnetic stirrer, and heated slowly. Previous works reported that the suitable temperature to maximize the solubilization of the CGC-FCT was 80°C and for the CGC-Com was 110°C [37]. The temperature was controlled using a digital thermo-regulator connected to the heating magnetic stirrer (Velp® Scientifica, Italy).

After the solubilization, the mixture was casted into a metal plate and then immersed on a coagulation bath at room temperature. The non-solvent used in the coagulation bath was deionized water, once the polymer is insoluble on it and ionic liquid is soluble. This step promotes the removal of ionic liquids from the polymeric structure. The formed membranes were dried at open space at room temperature for 5 to 7 days. If the mixture could not form a film, it is more suitable to form a hydrogel and by that, when finished the 24 h coagulation bath, the mixture was put into desiccators and leave it for 2 weeks. This step was done to confer a certain percentage of humidity to the hydrogel. The different percentages of water activity tested are described at the Table 2.2 [38].

Table 2.2 - Different water activities used at the desiccators [38].

Salt	a_w
CH ₃ COOK	0.216
Mg(NO ₃)	0.514
NaCl	0.751
KNO ₃	0.923

2.5 Chitin-Glucan Complex Mixtures Characterization

Before the phase inversion method, the mixtures of biopolymer - ionic liquids were characterized in terms of their sugar composition.

2.5.1 Chitin-Glucan Complex Mixtures Sugar Composition

Same procedure described at 2.3.1 was done to the characterization of 5 mg samples of CGC + ILs mixtures.

2.6 Chitin-Glucan Complex Films Characterization

The CGC films were characterized in order to understand their inherent properties. First, a sugar composition and thermal test were performed to the films produced. Then, a Scanning Electron Microscope (SEM) analysis, a contact angle measurement, a swelling test and a permeability test were executed to understand some features of their structure. A puncture test and an adhesion measurement were also performed to understand some mechanical properties of the films.

2.6.1 Films Sugar Composition

Same procedure described at 2.3.1 was done to the characterization of 5 mg samples of CGC films.

2.6.2 Thermal Properties

Same procedure described at 2.1.1.4 was done to the characterization of CGC films.

2.6.3 SEM Analysis

To understand the morphological structure of the polymeric films, they were analyzed by an emission electron microscope, JSM-7001 F (Jeol, Germany), operated with an intensity of 5 kV, at Instituto Superior Técnico, Universidade Técnica de Lisboa. This microscope allowed the observation and characterization of heterogeneous organic and inorganic materials at the scale of micro (10^{-6}) to nano (10^{-9}) meters.

The samples, with an area of 20 x 20 mm, were cut in a liquid nitrogen environment to have a clean surface and then were impregnated with a thin layer of gold particles to facilitate the conduction of the electron beam.

2.6.4 Contact Angle Measurements

The contact angle was measured by the sessile drop method, where a drop of distilled water was deposited manually on the polymeric surface by a small syringe. 10 images were acquired by the software and tangent was determined by fitting the drop shape to know mathematical function. The measurements were executed immediately after the drop falls on the surface. The instrument used was a KSV Cam 110 (KSV Instruments Ltd, Finland).

2.6.5 Swelling Tests

The swelling test is a technique that consists on measuring the amount of a certain liquid that a membrane can absorb. In this case distilled water was used. The membranes produced were cut into 1 x 1 cm² square-shaped samples and their weight and thickness (Elcometer, England) were measured. The samples were immersed in water and, after 24h, were withdrawn from water and measured their weight and thickness. This test occurred in a room at 30°C. To calculate the swelling of the membranes, the following equation was applied:

$$Swelling (\%) = \frac{m_{wet} - m_i}{m_i} \times 100 \quad \text{Eq. 2.3}$$

Where m_{wet} is the weight (g) of the wet membrane and m_i is the initial weight (g) of the dry membrane.

2.6.6 Permeability Tests

Permeability tests using the gases O₂, N₂ and CO₂ were performed in order to understand the capability of the films to permeate gases. Permeability tests were performed as represented in Figure 2.1. This equipment was composed by a stainless steel cell with two identical compartments separated by the membranes. The set-up is submerged in a thermostatic bath at 30°C. The temperature was regulated by a temperature controller (Haake, Germany). As depicted in Figure 2.1, the feed and permeate compartment were connect with two pressure indicators (Druck, England), which were connected to a data acquisition board, to observe the data in real time.

In a first step, a calibration procedure was performed by using a PDMS membrane (*Specialty Silicone Products*, USA) with known permeability to a specific gas, 2.08 x 10⁻¹⁰ m²/s, in this case N₂ (Praxair, USA) was used. By the data collected, it was possible to calculate the geometry parameter, β , which is a characteristic of the experimental cell used, through the following equation [38]:

$$\frac{1}{\beta} \times \ln \frac{\Delta p_0}{\Delta p} = P \times \frac{t}{l} \quad \text{Eq. 2.4}$$

Where β is a geometric parameter of the cell (cm^{-1}), Δp_0 is the difference in the pressure between the feed compartment and permeate compartment at $t = 0$ s (bar), Δp is the difference in the pressure between the feed compartment and permeate compartment along time (bar), P is the permeability value (cm^2/s), t is time (s) and l is the membrane thickness (cm).

The ideal selectivity between two gases is given by equation 2.5:

$$\alpha_{A/B} = \frac{P_A}{P_B} \quad \text{Eq. 2.5}$$

Where P_A is the permeability value of gas A (cm^2/s) and P_B is the permeability value to gas B (cm^2/s).

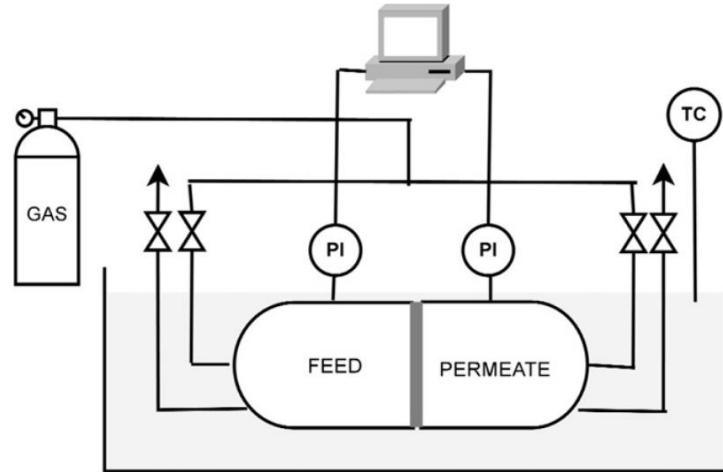


Figure 2.1 – Scheme of experimental set-up for measuring the pure gas permeability of the CGC films, where TC is Temperature Controller and PI is Pressure Indicator [39].

2.6.7 Mechanical Properties

A puncture stress test was carried out to understand the mechanical properties of the films produced, using a TA-Xt plus (Stable Micro Systems, England) texture analyzer. These measurements were performed at room temperature, $20 \pm 2^\circ\text{C}$.

The samples, with dimensions of 20 x 20 mm, were immobilized on a designed base with a 10 mm diameter hole. The samples were compressed at a speed rate of 0.5 mm/s and punctured through

the hole with cylindrical probe with 2 mm diameter. The puncture stress (τ_p) was expressed as the ratio of the puncture force (F_p) and the probe area (A_p) by the equation below:

$$\tau_p = \frac{F_p}{A_p} \quad \text{Eq. 2.4}$$

Where τ_p is a puncture stress (Pa), F_p is the puncture force (N) and A_p is the probe cross sectional area (m^2). This test also allows the determination of the elongation by the following equation:

$$\varepsilon_p = \frac{L_f - L_i}{L_i} \times 100 \quad \text{Eq. 2.5}$$

Where ε_p is a puncture elongation, L_f and L_i are the final and initial length (m), respectively.

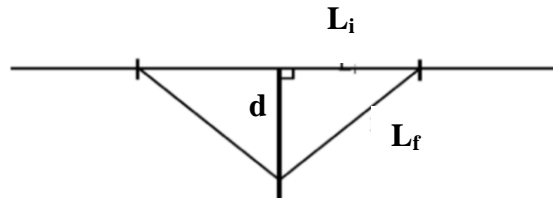


Figure 2.2 - Puncture test scheme.

In Figure 2.2 is shown a schematic representation of the puncture test, where the parameter L_f refers to the film final elongation and was calculated based on the distance measured by the probe, d , demonstrated by Equation 2.6. L_i is referred to the film initial position.

$$L_f^2 = d^2 + L_i^2 \Leftrightarrow L_f = \sqrt{d^2 + L_i^2} \quad \text{Eq. 2.6}$$

2.6.8 Adhesion Test

Pork skin was bought from a butcher's to be used as soft tissue in the bonding strength measurement. The skin was cut into $2 \times 2 \text{ cm}^2$ square-shaped pieces and firmly attached to metal testing holders with a matching surface area. Samples with the same square size of the pieces were spread uniformly between the two skin layers and the assembly was compressed with a constant force of 2 N for 5 min, as Figure 2.3 shows. Afterwards, the parts of the joint were strained axially at a constant velocity of 3 mm/min until separation was observed. The adhesion property was measured using a TA-Xt plus (Stable Micro Systems, England) [40].

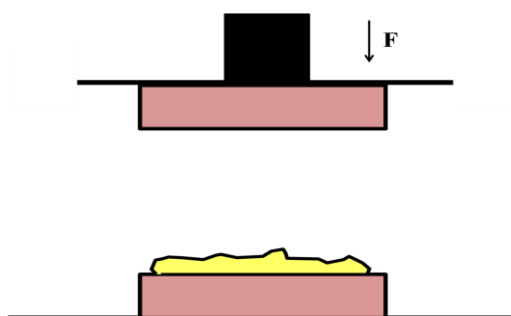


Figure 2.3 – *In Vitro* bonding strength measurement scheme, where the pork skin is represented by the pink square and the samples are represented by the yellow form. The direction of the force applied in the samples is demonstrated by the arrow.

2.7 CGC Hydrogels Characterization

Regarding the characterization of the hydrogels prepared, their composition, thermal properties, SEM, rheology behavior and adhesion property were evaluated.

2.7.1 Hydrogels Sugar Composition

Same procedure described at 2.3.1 was done to the characterization of 5 mg samples of CGC hydrogels.

2.7.2 Thermal Properties

Same procedure described at 2.1.1.4 was done to the characterization of CGC hydrogels.

2.7.3 SEM Analysis

Same procedure described at 2.6.3 was done to CGC hydrogels square 5 x 5 mm area samples.

2.7.4 Rheology Tests

Rheology tests were performed at Instituto Superior de Agronomia, Universidade de Lisboa, under supervision of Professor Vítor Alves, using a rheometer Haake Mars[™] II (Thermo Scientific, Germany) with a corrugated plate-plate geometry with a 20 cm of diameter. Stress sweeps were performed at constant frequency, 1 Hz, in order to ensure that the frequency sweeps were performed within the linear viscosity region. A tension of 10 Pa was used in all frequency sweeps performed, determining the dependence of the elastic (G') and viscous (G'') modules in relation to the frequency.

2.7.5 Adhesion Test

Same procedure described at 2.6.8 was done to the bonding strength measurements of CGC films.

3. Results and Discussion

In this thesis, the potential of using Chitin-Glucan Complex (CGC) as a wound treatment material for Chitin-Glucan Complex (CGC) was evaluated. Different biocompatible cholinium based ionic liquids were selected to dissolve two different types of CGC biopolymers. Several tests were performed in order to conclude which ionic liquid is more suitable to dissolve the polymer and which polymeric structure is more appropriate to become a wound dressing.

3.1 Ionic Liquids Characterization

3.1.1 Ionic Liquids Water Content and Density

The cholinium based ionic liquids used in this work were firstly characterized in terms of its water content and density. The results are shown at Table 3.1.

Table 3.1 - Water content and density of the cholinium based ionic liquids.

Ionic Liquids	Water Content (%)	Density (g/ cm³)
Choline Acetate	11.29 ± 0.002	1.08 ± 0.0030
Choline Propionate	9.30 ± 0.002	1.06 ± 0.0001
Choline Isobutanoate	8.31 ± 0.005	1.04 ± 0.0011
Choline Hexanoate	14.00 ± 0.008	1.03 ± 0.0001

Choline hexanoate showed the higher water content value of all ionic liquids used in this study. However, the results obtained were much higher when compared with the ones obtained by Muhammad *et al*, where the values were below 1% [41]. This could be explained by differences in the synthesis method used in the two works, where the ILs studied by Muhammad *et al* were possibly subdued to a more drier step than the ones synthesized for the present work. A higher presence of water could lead to a alteration in some properties of the ILs, namely the viscosity, which will be discussed in the next section [42].

The density is related with the molar mass of the ions and ILs with heavier atoms in their composition are in general denser than the ones with lighter atoms [42]. With the increase in the alkyl chain length of the anion, the density values obtained should present an increase. Here, it was observed that density values were maintained which might predicts that the alkyl chain length did not

have a significantly impact. Important to mention that although there is a decreased in density values at Table 3.1, this happened at centesimal values which had not significant influence.

3.1.2 Viscosity Measurements

A viscosity study was carried out for all ionic liquids used on this work, varying the shear rate at three different temperatures, 30°C, 80°C and 110°C and measuring the shear stress, where the slope represents the viscosity values demonstrated on Table 3.2. Additional data is shown at Appendix II and Appendix III.

Table 3.2 - Viscosity and activation energy of the ionic liquids used.

Ionic Liquid	Viscosity (Pa.s)			Ea (kJ/ mol)
	30°C	80°C	110°C	
Choline-Acetate	0.0785	0.0225	0.0145	8.97
Choline-Propionate	0.0606	0.0202	0.0120	8.49
Choline-Isobutanoate	0.0837	0.0225	0.0150	9.19
Choline-Hexanoate	0.1428	0.0397	0.0217	9.88

The ionic liquids have a linear correlation between the shear stress and the shear rate, which corresponds to a Newtonian fluid behavior. Taking this into account, it was expected to have a decrease in the viscosity values, featured on Table 3.2, with the increasing temperature [42]. In addition, it was observed an increase of the viscosity values alongside with the alkyl chain length, except for the choline-propionate. This increasing in viscosity was also expected, once the van der Waals interactions in the alkyl chains were augmented in the different ionic liquids, which affects their viscosity [43-44].

For choline-acetate, a value of viscosity obtained was 0.0784 Pa.s at 30°C. This result was not expected when compared with Cândido data that obtained a viscosity value of 0.1860 Pa.s, for the same ionic liquid and same temperature. As stated in the section 3.1.1, the water content in the IL could alter the viscosity properties of the solutions. Once the water content measured in this work was 11.3% and in Cândido data was 8.8%, a slight increasing in the water amount present in the IL could lead into a significant decrease in the viscosity value. This correlation might be applied for the others ILs, once Muhammand *et al* data showed a water content for the same ILs below 1% and a higher viscosity values compared with the ones obtained [41-42, 45].

In order to correlate the viscosity with the temperature, a Arrhenius equation was used:

$$\eta = \eta_0 \cdot e^{-\frac{E_a}{RT}} \quad \text{Eq. 3.1}$$

Where η is the apparent viscosity in Pa.s at a specific shear rate, η_0 is the frequency factor in Pa.s, E_a is the activation energy in KJ/mol, R is the gas constant in KJ/mol.K and T is temperature in K.

A logarithmic equation based on Arrhenius model was used to determine the activation energy:

$$\ln \eta = \ln \eta_0 - \frac{E_a}{RT} \quad \text{Eq. 3.2}$$

As observed in Table 3.2, there is an increase in the E_a values as long as the anion size is higher, except for the choline-propionate sample. The other values were expected, since a higher E_a value represents a difficulty for the ions to move past each other due to their dimension.[46] Comparing with other cholinium-based ionic liquids, these results were much lower than the expected, even with similar water content. This could show that the ionic liquids studied in this work do not establish strong hydrogen bonds in aqueous solution [46].

3.2 Chitin-Glucan Complex Sugar Composition

The sugar composition was determined for: i) samples of CGC-Com and CGC-FCT polymers, ii) mixtures of both CGC polymers before the phase inversion method, iii) CGC films and hydrogels. The composition of sugars, glucose, mannose and glucosamine, in all samples is described in Table 3.3. The values displayed in Table 3.3 are related to the samples quantity. The composition of glucose and mannose refers to the quantity of glucans and the composition of glucosamine to the quantity of chitin present in the CGC polymer [18].

On the specification of KiOnutrime-CG™, Kitozyme states that the ratio of glucan-chitin produced by *A.niger* is about 65 : 25 to 40 : 60 [16]. It was possible to confirm that the ratio obtained for CGC-Com standed within the specification range for this product. Although glucose is the predominant sugar constituent of the cell wall of *A.niger*, it was the CGC-FCT polymer, produced by *K.pastoris* that showed a higher ratio of this sugar. Moreover, it was observed that these two polymers

showed substantial differences in their composition, once CGC-Com had a 50 : 50 Glucan : Chitin ratio and CGC-FCT a 81 : 19 Glucan : Chitin ratio.

Analyzing first the data for CGC-Com, it was possible to observe that for the CGC-Com mixtures before the phase inversion method there was a significant loss in the chitin ratio, except when used the choline hexanoate IL, where there was any substantial difference. These results were not expected at all, once the sugars composition should not be affected by the ILs addition. When the mixtures form the films, after passed by the phase inversion method, the results obtained vary significantly. For choline acetate and choline propionate it was observed a loss in glucans ratio comparing to CGC-Com ratio. Relative to the other ILs, the opposite occur, where the loss of chitin was more prominent with choline isobutanoate.

The data obtained for CGC-FCT, showed the same unexpected results to the mixtures before the phase inversion method, where choline acetate and choline hexanoate showed more discrepant values. After the phase inversion method, data showed the same loss on the chitin ratio for the same ILs. Plus, with hydrogels, chitin ratio loss was also observed.

In the dissolution process using ILs, the CGC could suffer some hydrolysis. Generally, there was a higher loss of chitin rather than glucan ratio for CGC-FCT. This could be explained, by the fact that the chitin fraction was more susceptible to be hydrolyzed by the ILs, rather than the glucans. Also, it could explain the low chitin ratio present in the polymeric structures produced using choline isobutanoate.

Additionally, the overall data did not demonstrate a correlation between the initial ratio and the ones obtained along the polymeric structures production steps. Once this sugar composition was only measured one time, a repeated assessment should be accomplished. Further studies, ash and protein quantification, should be also perform, in order to evaluate the presence of contamination at biopolymers structures, once these compounds might influence the sugar measurements and X-Ray Diffraction (XRD) and solid state Nuclear Magnetic Resonance (NMR) tests could also be measured in order to identify the structural characteristics of these compounds and materials.

Table 3.3 – Sugar constituents in CGC polymers and polymeric materials.

	Samples	Glucose (ppm)	Mannose (ppm)	Glucosamine (ppm)	Ratio Glucan and Chitin
CGC Polymers	CGC-Com	218.40	8.40	225.49	50 : 50
	CGC-FCT	270.44	6.01	65.52	81 : 19
CGC Mixtures before Phase Inversion Method	Choline Acetate CGC-Com	42.51	0.92	29.32	60 : 40
	Choline Propionate CGC-Com	21.89	0.59	17.88	56 : 44
	Choline Isobutanoate CGC-Com	44.33	1.36	26.76	63 : 37
	Choline Hexanoate CGC-Com	16.99	0.48	17.89	49 : 51
	Choline Acetate CGC-FCT	21.74	0.35	11.74	65 : 35
	Choline Propionate CGC-FCT	29.40	0.36	5.15	85:15
	Choline Isobutanoate CGC-FCT	13.88	0.26	3.67	79 : 21
	Choline Hexanoate CGC-FCT	31.30	0.40	5.06	86 : 14
CGC Films	Choline Acetate CGC-Com	51.60	0.66	65.09	45: 55
	Choline Propionate CGC-Com	78.47	0.95	120.22	40 : 60
	Choline Isobutanoate CGC-Com	46.74	0.31	1.14	98 : 2
	Choline Hexanoate CGC-Com	46.93	0.77	37.87	56 : 44
	Choline Acetate CGC-FCT	50.85	0.69	6.25	89 : 11
	Choline Propionate CGC-FCT	60.68	0.71	11.68	84 : 16
	Choline Hexanoate CGC-FCT	49.77	0.72	3.47	94 : 6
Choline-Isobutanoate CGC-FCT Hydrogels	Hydrogel with $a_w = 0.216$	74.97	3.30	7.50	91 : 9
	Hydrogel with $a_w = 0.514$	134.20	2.72	11.09	93 : 7
	Hydrogel with $a_w = 0.751$	210.99	6.27	16.31	93 : 7
	Hydrogel with $a_w = 0.923$	82.44	2.89	8.34	91 : 9

3.3 Chitin-Glucan Complex Thermal Properties

Thermogravimetry was used in this work to observe the variation of mass materials in a range of temperatures. However, these results are not shown in this thesis work due to a delay in the analysis.

3.4 Chitin-Glucan Complex Films Characterization

3.4.1 SEM Analysis

The SEM technique allowed the observation of films' top surface and their cross section. Unfortunately, the majority of the samples used for this analysis did not react well to the pre-treatment submitted before the analysis started. This affected especially the cross-section images obtained, once the films structures were distorted. Figure 3.1 display images of different films obtained using CGC-Com polymer.

The top images showed that choline acetate CGC-Com film had the most random structure pattern and choline propionate CGC-Com, choline isobutanoate CGC-Com and choline hexanoate CGC-Com films showed a smoother structure pattern. However, choline isobutanoate CGC-Com and choline hexanoate CGC-Com films presented some pores at surface, specially the last one referred. In terms of the cross-section images, it could be observed that the choline acetate CGC-Com film had the structure distorted due to the pre-treatment it was submitted, and the rest of the films had a dense structure, with the exception of choline hexanoate that showed some pores along their structure.

Figure 3.2 shows the top surface image results obtained for the different films using the CGC-FCT polymer, where choline acetate CGC-FCT and choline hexanoate CGC-FCT films had some bubbles in it surface. Although the phase inversion method promotes the removal of ionic liquids, it is possible that a residual quantity could stay in the polymeric structure. The presence of these bubbles could represent an excess of IL present in the structure that was heated by the electron beam. Although choline acetate CGC-FCT and choline propionate CGC-FCT presented similar glucan : chitin ratio, structurally there are major differences, once choline propionate CGC-FCT film showed a smoother structure pattern. For the cross- section images, it was shown that choline acetate CGC-FCT film had its structure distorted, by the pre-treatment and, choline propionate CGC-FCT film presented a dense structure. Plus, due to the pre-treatment a cross-section image of choline propionate film was not able to be taken.

In section 3.4.4, a permeability test was done to the films that present a smoother and dense structure viewed by the SEM images [47].

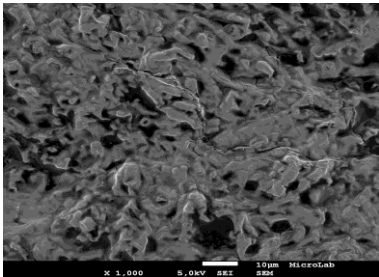
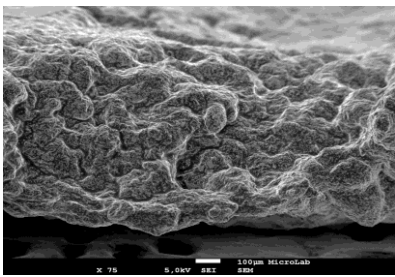
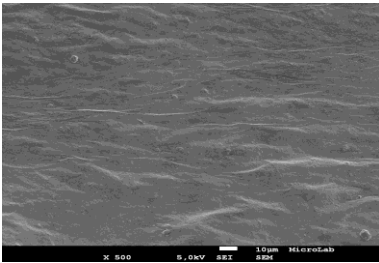
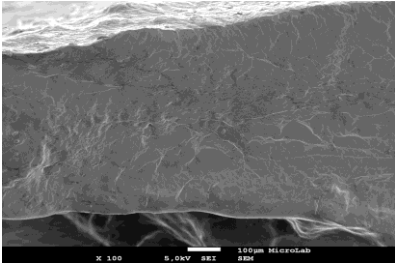
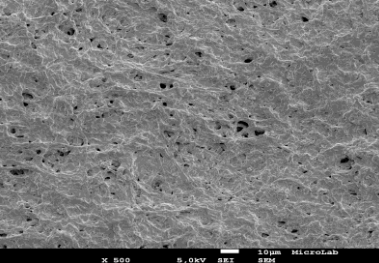
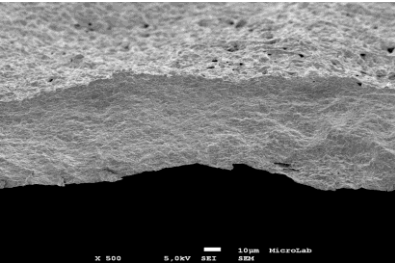
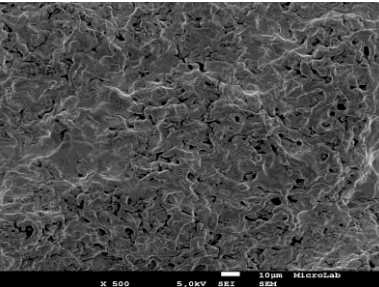
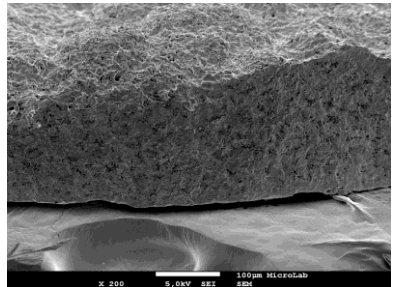
Sample	Top Surface	Cross-section
Choline Acetate CGC-Com		
Choline Propionate CGC-Com		
Choline Isobutanoate CGC-Com		
Choline Hexanoate CGC-Com		

Figure 3.1 - SEM images of top surface and cross-section of CGC-Com films. Images amplification for top surface and cross-section are, respectively: Choline Acetate CGC-Com – x1000 and x75; Choline Propionate CGC-Com – x500 and x100; Choline Isobutanoate CGC-Com – x500 and x500; Choline Hexanoate CGC-Com – x500 and x200.

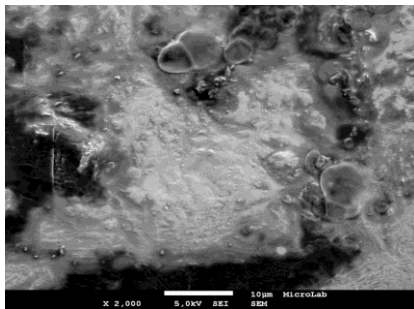
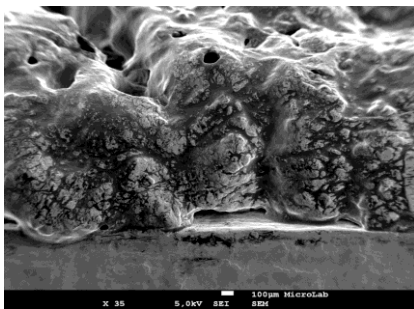
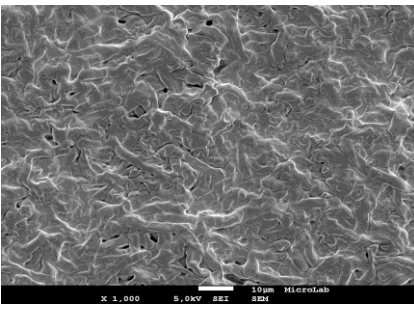
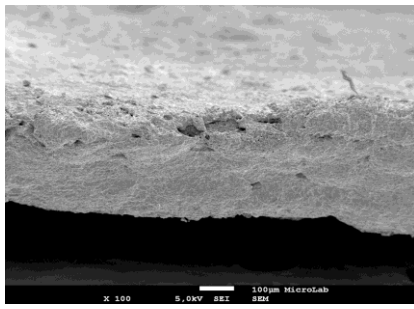
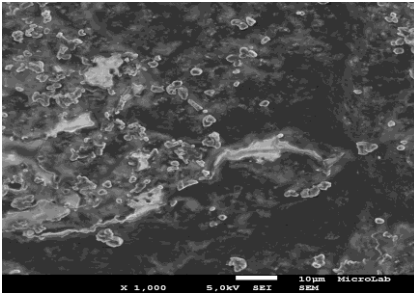
Sample	Top Surface	Cross-section
Choline Acetate CGC-FCT		
Choline Propionate CGC-FCT		
Choline Hexanoate CGC-FCT		

Figure 3.2 - SEM images of top surface and cross-section of CGC-FCT films. Images amplification for top surface and cross-section are, respectively: Choline Acetate CGC-FCT – x2000 and x35; Choline Propionate CGC-FCT – x1000 and x100; Choline Hexanoate CGC-FCT – x1000.

3.4.2 Contact Angle Analysis

A material wettability could be determined by the measurement of water contact angle. In case the solid surface is hydrophobic, the contact angle formed by the water will be higher than 90°.[48] The results obtained are presented in Figure 3.3. Only the samples containing CGC-Com polymer were used due to their inner structure rigidity, while CGC-FCT samples that presented a softer structure were not suitable to perform this test.

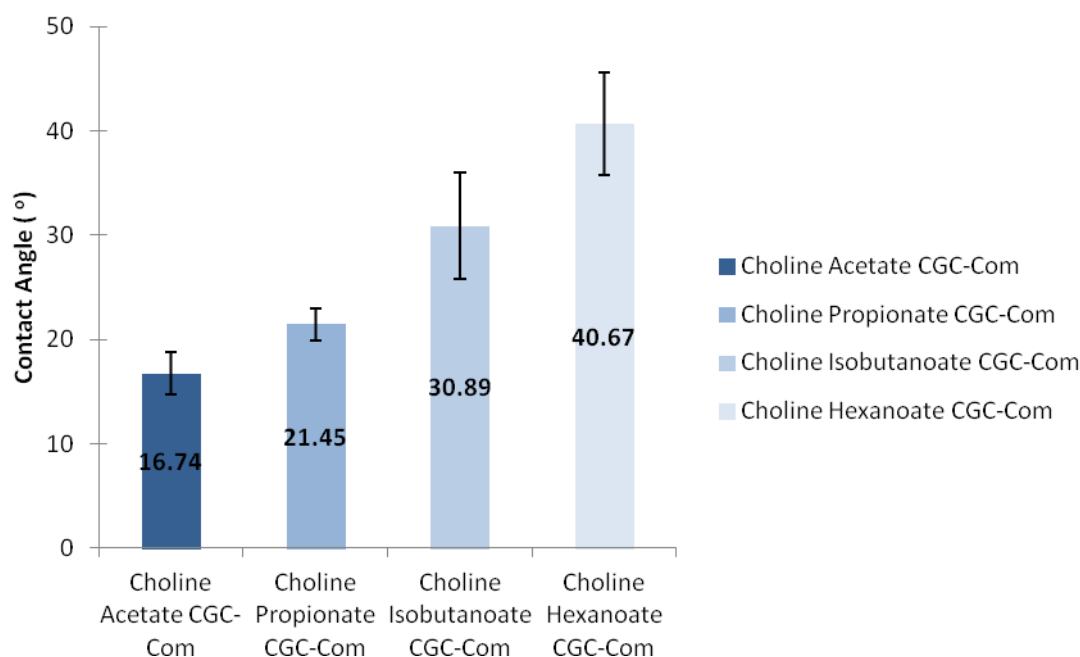


Figure 3.3 - Contact angle of CGC-Com films produced by different ionic liquids.

Figure 3.3 reveals the hydrophilic nature of all samples, once the contact values are lower than 90° [48]. This could also be correlated by the fact that a residual quantity of IL is still in the polymeric structure. In this way, choline acetate is an IL very hydrophilic and, although all samples present a hydrophilic nature, it is observed that an increase of ILs chain length could affect the samples hydrophilicity.

3.4.3 Swelling Tests

In order to understand the capacity of the films produced interacts with water, a swelling test was performed, where the results obtained are in Table 3.4. Typically, a polymer has a free volume in their structure which can be occupied by solvent molecules. Once the solvent enters the polymer structure, an interaction between polymer and solvent starts to occur. The polymer chains start to have a repulsion interaction resulting on a swell by the polymer molecules [49].

Firstly, Choline Acetate CGC-Com and Choline Propionate CGC-Com films showed a negative weight percentage. This could be related to a residual IL presented in the structure that was dissolved by the water, leading to a decrease in the polymeric material weight. Choline Isobutanoate CGC-Com presents a higher weight percentage value that could be related with the pores presented in their dense structure, as it can be seen in SEM images at section 3.4.1. This could be connected to the fact that this structure has more free volume for the water entry. However, Choline Hexanoate CGC-Com porous membrane did not almost have any swell by its structure, once the value is almost null.

This could be correlated by the fact that choline hexanoate is the most hydrophobic IL from all samples.

Table 3.4 – Swelling results of CGC films.

Films	Weight (%)
Choline Acetate CGC-Com	-15.90
Choline Propionate CGC-Com	-1.17
Choline Isobutanoate CGC-Com	56.25
Choline Hexanoate CGC-Com	0.39
Choline Acetate CGC-FCT	43.41
Choline Propionate CGC-FCT	71.66
Choline Hexanoate CGC-FCT	40.41

In terms of CGC-FCT films, all samples showed high weight percentage value, where choline propionate CGC-FCT stands out. Different polymers sources could lead into some structure differences between them. CGC-FCT might have a structure that promotes the interaction between its constituents and the solvents. Choline propionate CGC-FCT has a swelling value of 71.66% and as it can be seen in Figure 3.3, in section 3.4.1, this film has a dense structure. This could be an interesting film feature, once it absorbed a percentage considerable of water, for a wound dressing since it can absorb wound exudates, preventing bacterial infection.

3.4.4 Permeability Tests

In order to understand gas transport properties of the CGC films prepared, a permeability test was performed. The gases used were N₂, O₂ and CO₂, once they are present in the atmosphere and, also, are important in the reparative skin processes, namely the last two gases. As stated in section 3.4.1 only the films with a dense structure were suitable to perform this test, however just two of them, Choline Propionate CGC-Com and Choline Hexanoate CGC-Com, had the size and rigidity needed to perform this analysis. The others films presented some fissures in their structure and for this reason it was not possible to carry out this measurement.

Using Equation 2.4, it was possible to calculate the permeability value. The results are shown in Table 3.5 for both films using N₂, O₂ and CO₂ gases, respectively.

Table 3.5 - CPC and CHC permeability values for N₂, O₂ and CO₂ gases and selectivity values of CO₂/N₂, CO₂/O₂ and N₂/O₂.

CGC Films	Permeability (Barrer)			Selectivity		
	N ₂	O ₂	CO ₂	$\alpha_{\text{CO}_2/\text{N}_2}$	$\alpha_{\text{CO}_2/\text{O}_2}$	$\alpha_{\text{N}_2/\text{O}_2}$
Choline propionate CGC-Com	3286.9	2409.6	3363.9	1.02	1.40	1.36
Choline hexanoate CGC-Com	46.4	4.1	215.9	4.65	52.66	11.32

From the results observed in Table 3.5, major differences were observed between the two samples used for this test. Choline propionate CGC-Com showed higher values for all gases permeability tests. This was expected since the SEM images showed that the choline hexanoate CGC-Com film had in their structure some pores, which facilitate the gases movement through the membrane. It was also shown that the choline hexanoate CGC-Com had a higher selectivity for each combination of gases, $\alpha_{\text{CO}_2/\text{N}_2}$, $\alpha_{\text{CO}_2/\text{O}_2}$ and $\alpha_{\text{N}_2/\text{O}_2}$. This results is concordant with the literature, once polymer membranes which are more permeable, have a tendency to become less selective [50].

However, these results when compared with others using a chitosan hydrogel membrane, for N₂ and CO₂, 3.42 Barrer and 166.7 Barrer, respectively, at 30°C and cellulose membrane, for O₂, 6.28 Barrer, at 25°C are much higher, except for the O₂ choline hexanoate CGC-Com permeation value [51, 52].

3.4.5 Mechanical Properties

The films prepared were characterized in terms of their mechanical properties, through a puncture test. The results obtained are in Table 3.6. For this test, only CGC-Com films were measured, due to their stronger structure.

Table 3.6 – Mechanical properties of commercial CGC films, where τ_p is the puncture stress and ϵ the puncture elongation.

Samples	Thickness (μm)	τ_p (kPa)	ϵ (-)	Normalization τ_p (kPa) per thickness (μm)
Choline Acetate CGC-Com	440	19.35	0.039	0.044
Choline Propionate CGC-Com	347	432.46	0.149	1.246
Choline Isobutanoate CGC-Com	428	299.75	0.134	0.700
Choline Hexanoate CGC-Com	249	480.30	5.356	1.928

A good film mechanically should have an adequate tensile strength and extensibility, in order to hold out external stress, maintain its integrity and act as a barrier. These are important properties for packaging and wound dressing areas [48, 52]. Analyzing the four deformations curves, exhibit in Appendix IV, and the data in Table 3.6, it can be observed that the choline hexanoate CGC-Com film had a higher puncture stress, 480.298 kPa.

The puncture stress and elongation at break are dependent on the membrane thickness, which could be normalized in a puncture measurement to have a better correlation. In terms of this data, the films with a higher thickness were the ones with a lower puncture stress (τ_p), where choline acetate and choline isobutanoate CGC-Com had a normalization value of 0.044 kPa/ μm and 0.700 kPa/ μm , respectively. Same observation was concluded by Ardiyanti, where the thickness value of laboratory CGC film, 124 μm , could sustain forces two times higher, compared to the commercial CGC film, with a thickness of 230 μm , which could refer to the elasticity and high mechanical strength that the films had for a good wound dressing, especially choline propionate and choline hexanoate CGC-Com [37, 54].

3.4.6 Adhesion Measurements

For the adhesion measurements, pork skin square samples were used as soft tissue, to mimic the human skin, in order to evaluate the adhesivity properties of the CGC films produced. A pre-test was made, where small quantity CGC film sample got compressed between two small pigskin fragments to observe the adhesivity of the sample. In this pre-test, all CGC-Com films were excluded from this measurement, since none adhesivity property was observed.

All CGC-FCT films were submitted to a constant force of 2 N, during 5 min, then the equipment register the maximum tension value that the samples resisted. These results are at Table 3.7.

Table 3.7 - Maximum tension values of CGC laboratory films for adhesion measurements.

Films	τ_{max} (kPa)
Choline Acetate CGC-FCT	2.36
Choline Propionate CGC-FCT	5.90
Choline Hexanoate CGC-FCT	10.41

The results showed that choline hexanoate CGC-FCT film had the higher bonding strength to the pork skin, 10.41 kPa, almost two times higher than choline acetate CGC-FCT film and five times

higher than choline acetate CGC-FCT film. Due to the conclusion taken from the pre-test made, films with a more dense structure demonstrated no adhesive property.

As it can be seen on the Figure 3.2 in section 3.4.1, the top surface and cross-section of the samples used on this test, choline acetate CGC-FCT had a random structure, such as choline hexanoate CGC-FCT structure film, where the first film had an excess of IL in their structure. Therefore, a higher ionic liquid quantity could affect the adhesive property of the film and explain the lowest value from all samples. Choline propionate CGC-FCT had a smoother surface than the others films, though it showed a very adhesive property.

Gelatin is a natural polymer derived from collagen, which is a promising candidate for tissue adhesives due to its inherent characteristics. The results obtained in the present work are very similar to the ones obtained from Shefy-Peleg *et al* work. Gelatin lowest and highest values for bonding strength were, about, 2 kPa and 10 kPa, respectively [40]. Also, the choline propionate and choline hexanoate CGC-FCT results were higher than the ones obtained by a commercial wound dressing, Evicel[®], 2.5 kPa. This comparison showed the potential CGC has for wound dressing, since has a natural property to adhere into a soft tissue.

3.5 CGC Hydrogels Characterization

3.5.1 SEM Analysis

The SEM technique allowed the observation of hydrogels' top surface. For these samples more conductive film was used, however the conduction of the electron beam did not occur always as desirable, once the gold layer did not stand at the hydrogels surface, due to its structure. In Figure 3.4 are the SEM images of the hydrogels produced in this work.

As it is possible to observe the top surface of all hydrogels at different water activities show an irregular and absence of a porous structure. For a wound dressing is suitable to have some porous structure, in order to be permeable to wound exudates. This can prevent the formation of an infection [55].

Hydrogel with $a_w = 0.514$ had the smoother surface and hydrogel with $a_w = 0.216$ and hydrogel with $a_w = 0.923$ were the most roughness surface. In the last two referred, some grains are observed in the images, which could be present due to a poor dissolution. This also could be related with their inner structure or to the vacuum environment that the samples were subdued in this analysis, since it is possible to form grains and it is not identified how the hydrogels react in this condition. In order to know if the vacuum plays an important factor in their formation, a more detailed test should

be taken into account, such Environmental Scanning Electron Microscope (ESEM), where the samples are examined in a high chamber pressure atmosphere of water vapor.

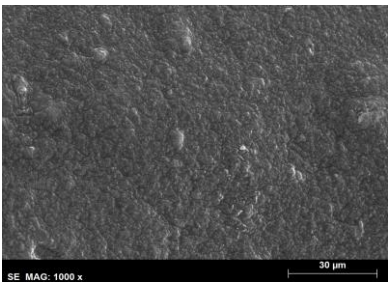
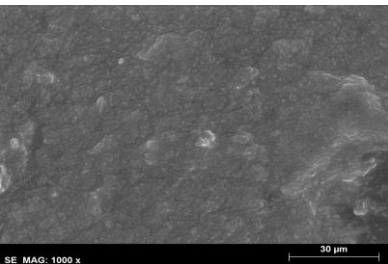
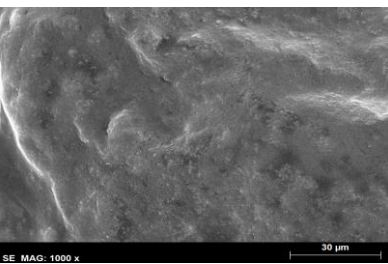
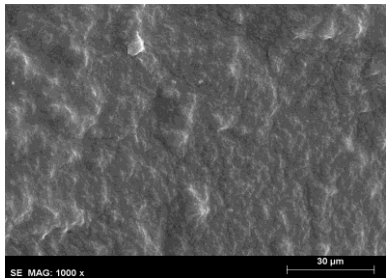
Sample	Top Surface
Hydrogel with $a_w = 0.216$	
Hydrogel with $a_w = 0.514$	
Hydrogel with $a_w = 0.751$	
Hydrogel with $a_w = 0.923$	

Figure 3.4 – SEM images of top surface of choline isobutanoate CGC-FCT hydrogels. Images amplification for top surface are: Hydrogel with $a_w = 0.216$ – x1000; Hydrogel with $a_w = 0.514$ – x1000; Hydrogel with $a_w = 0.751$ – x1000; Hydrogel with $a_w = 0.923$ – x1000.

3.5.2 Rheology Tests

3.5.2.1 Dynamic State Measurements

In this study, strain sweep measurements were performed in order to obtain the linear viscosity region at low frequencies for all CGC hydrogels samples. For this measurement, a tension was selected from a stress sweep done previously.

In Figure 3.5, it is observed that all CGC hydrogels produced in this work present similar mechanical spectrum, where the elastic modulus (G') is higher than the viscous modulus (G''), with a slight variation with the frequency. This behavior is generally attributed to structures similar to a strong gel [56]. These results envisage that the hydrogels rheological behavior is suitable for a material with applications in the wound dressing area, as they possess both good elastic and viscous properties, being the first one that with a higher contribution.

Similar observations were made in studies measuring chitosan rheological behavior. An identical conclusion was taken for this polymer, however G' was higher than G'' by two orders of magnitude, implying a stronger gel than the one produced in this work [56-57].

Once the strong or weak property of a hydrogel is defined by the difference between the elastic (G') and viscous (G'') modulus, it was the hydrogel with 0.514 and the hydrogel with 0.751 water activities that expressed a major difference between these parameters, meaning that these two were the stronger gels produced. On the other hand, hydrogel with $a_w = 0.923$ showed the lowest values for both G' and G'' , meaning that from all hydrogels produced it is the weaker. However it should be taken into account that, with the increase of frequency, the viscous modulus (G'') tends to approximate the elastic modulus (G'), meaning that at high frequencies this property tends to decrease significantly.

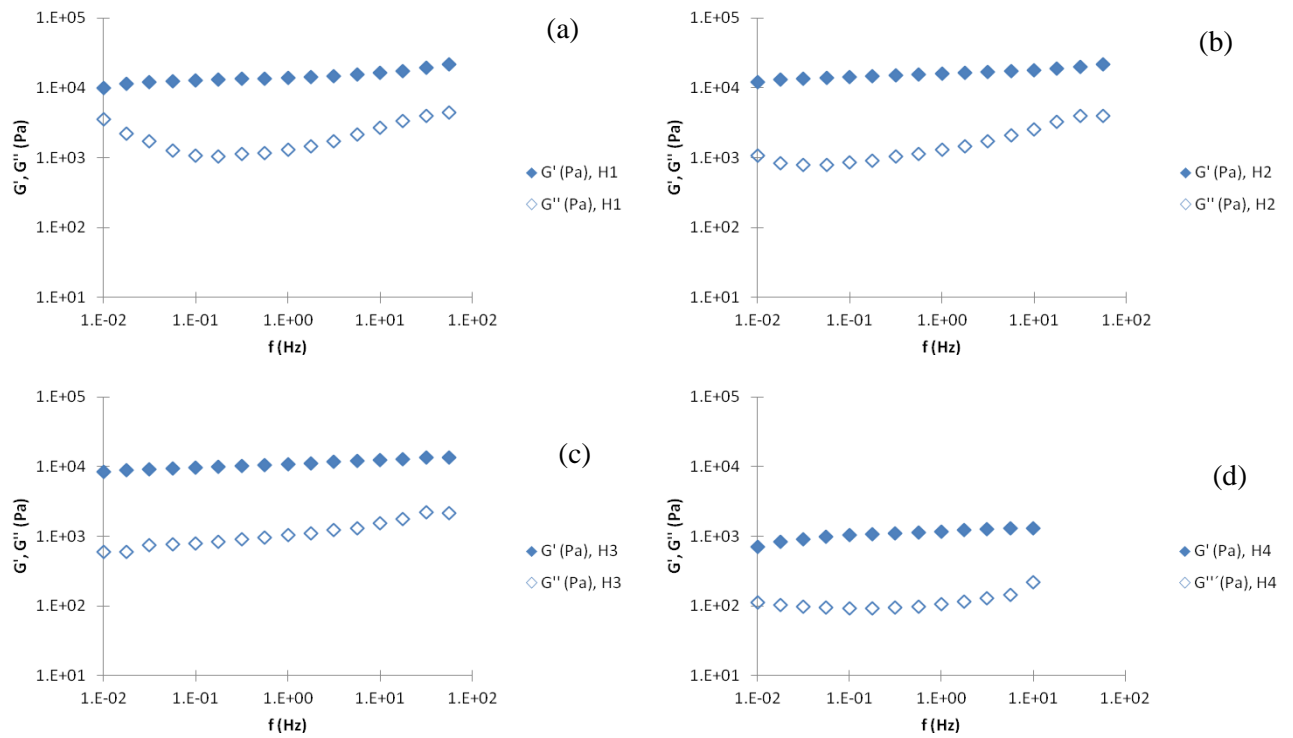


Figure 3.5 - Frequency sweeps for CGC hydrogels, (a) H1 – hydrogel with $a_w = 0.216$, (b) H2 – hydrogel with $a_w = 0.514$, (c) H3 – hydrogel with $a_w = 0.751$ and (d) H4 – hydrogel with $a_w = 0.923$.

3.5.3 Adhesion Measurements

All hydrogels were submitted to a constant axial compression force of 2 N, during 5 min, after which an axial tensile force was applied, and then the equipment registered the maximum tension values that the samples resisted before skin layers separation. These results are shown in Table 3.8.

Table 3.8 - Maximum tension values of CGC laboratory hydrogels for adhesion measurements.

Hydrogels	τ_{\max} (kPa)
Hydrogel with $a_w = 0.216$	2.01
Hydrogel with $a_w = 0.576$	13.00
Hydrogel with $a_w = 0.751$	8.94
Hydrogel with $a_w = 0.923$	16.98

The test results showed that the hydrogel with higher water activity had the higher tension value from all samples, although there is no linear correlation with the increase of the water activity in hydrogels and their maximum tension values.

The top surface SEM images on Figure 3.5, in section 3.5.1, showed an identical morphologic structure among hydrogel with $a_w = 0.514$ and hydrogel with $a_w = 0.923$, which were the two samples with the highest tension values of 13.00 kPa and 16.98 kPa, respectively. Hydrogel with $a_w = 0.216$ showed a more random structure than the others, which could imply a structure that had more difficulties to interact with the soft tissue, once it has the lowest value, 2.01kPa. It was expected that the hydrogel with $a_w = 0.751$ had a higher maximum tension value, once the dynamic state measurement, section 3.5.2, showed that this hydrogel was the one that more showed characteristics of a strong gel.

The promising polymer, gelatin, for wound close applications had, for this test, values from about 2kPa to 10 kPa, which is the range of the obtained results, although hydrogen with $a_w = 0.216$ and hydrogen with $a_w = 0.923$ showed a higher bonding strength value than 10 kPa [40]. This comparison demonstrated the adhesion property of CGC-FCT in the hydrogel form, however this could not be particularly a good feature for a wound dressing. A high value of adhesion could mean that the dressing is more difficult to remove, which could cause trauma to the tissue.

4. Conclusion

The main goals of this work was to obtain CGC based polymeric structures using biocompatible ionic liquids and study their potential in the biomedical field, as wound treatment materials. Different characterization techniques were selected and tested considering the characteristics that an ideal wound dressing should have.

All the choline-based ionic liquids used in this work were capable to dissolve the two CGC polymers producing polymeric structures with different physic-chemical properties. The polymeric structure obtained when using choline acetate ionic liquid as dissolution agent has shown unstable behavior, probably due to the hydrophilic character of this IL. Choline propionate and choline hexanoate were the ILs that prepared polymeric structures with interesting properties in the majority of the characterization techniques studied. It was also observed that when using choline isobutanoate the polymeric structures obtained, gel and films, contained the lowest amount of chitin in their structure, which can explain the non-ability to produce a stable film.

The total mass obtained for CGC-FCT was 18.88g. This polymer showed a much higher glucan ratio than the CGC-Com, however their polymeric structures were more fragile than the ones produced by CGC-Com. In order to obtain a more cohesive film, a glucan : chitin ratio should be more equivalent.

The ionic liquids that dissolved and produced the polymeric structures of both polymers with best features for a wound dressing were choline propionate and choline hexanoate. These two ILs produced films showed a high gas permeability, choline propionate, and high selectivity of CO_2/O_2 , choline hexanoate, using both CGC-Com. Also, the polymeric structure dissolved by choline propionate showed a great swelling capacity, obtained a value of 71.66%, where the polymeric structure dissolved by choline hexanoate showed also a high value of 40.41%. In terms of adhesivity, choline hexanoate CGC-FCT showed a high value of 10.41 kPa and choline propionate, 5.90 kPa, which in both cases showed the natural adhesivity property of CGC. Choline isobutanoate was also an interesting ionic liquid tested, once it was not able to produce a polymeric structure in a film form for CGC-FCT. The hydrogels produced were concluding to have some strong gel properties and strong adhesivity values.

In this work, the films using commercial CGC had shown an advantage in term of the films using laboratorial CGC, once the membranes produced were much fragile than the ones produced by CGC-Com, where presented some fissures. Although there were more results obtained for CGC-Com, CGC-FCT also present some features that, once their polymeric structures production is optimized, could be used as a wound treatment material.

5. Future Work

For future work there are some tests that can be performed, in order to further evaluate the potential and promise of CGC polymeric materials as wound dressings. Some examples of future improvements are:

- Analyze the content of the ash and proteins in the two polymers, in order to evaluate the purity percentage, namely for CGC-FCT;
- Analyze the films composition by XRD (X-ray diffraction) or NMR (Nuclear Magnetic Resonance), in order to obtain more information about the form of chitin (either it is in the form of α or β), well as the interactions between the polymer and ionic liquid before and after the phase inversion method;
- Since the films obtained when using the CGC-FCT polymer were not stable, hydrogel production should be carried out;
- Optimize the dry procedure, in a controlled atmosphere, with a constant temperature (e.g. 30°C) and controlled humidity, to avoid fissures in the films;
- Evaluate the water vapor permeability to the samples;
- Perform an Environmental Scanning Electron Microscope (ESEM) to the hydrogels samples, to know if the vacuum environment formed the grains observed at SEM analysis or if these grains are part of their structure;
- Perform *In vitro* and *In vivo* tests to measure the antimicrobial activity and the regenerative healing properties of the CGC-based polymeric materials as a wound dressing.

6. References

- [1] Sang Hyun Lee; Minoru Miyauchi; Jonathan S. Dordick e Robert J. Linhardt, "Preparation of Biopolymer-Based Materials Using Ionic Liquids for the Biomedical Application," *Am. Chem. Soc.*, vol. 10, pp. 115–134, 2010.
- [2] P. Yadav, H. Yadav, V. G. Shah, G. Shah, and G. Dhaka, "Biomedical biopolymers, their origin and evolution in biomedical sciences: A systematic review," *J. Clin. Diagnostic Res.*, vol. 9, no. 9, pp. 21–25, 2015.
- [3] A. C. a Wan and B. C. U. Tai, "CHITIN--a promising biomaterial for tissue engineering and stem cell technologies.," *Biotechnol. Adv.*, vol. 31, no. 8, pp. 1776–85, 2013.
- [4] R. Jayakumar, M. Prabakaran, P. T. Sudheesh Kumar, S. V Nair, and H. Tamura, "Biomaterials based on chitin and chitosan in wound dressing applications.," *Biotechnol. Adv.*, vol. 29, no. 3, pp. 322–37, 2011.
- [5] E. Atkins, "Conformations in polysaccharides and complex carbohydrates," *J. Biosci.*, vol. 8, pp. 375–387, 1985.
- [6] C. K. S. Pillai, W. Paul, and C. P. Sharma, "Chitin and chitosan polymers: Chemistry, solubility and fiber formation," *Prog. Polym. Sci.*, vol. 34, no. 7, pp. 641–678, Jul. 2009.
- [7] M. Rinaudo, "Main properties and current applications of some polysaccharides as biomaterials," vol. 430, no. April 2007, pp. 397–430, 2008.
- [8] M. Rinaudo, "Chitin and chitosan: Properties and applications," *Prog. Polym. Sci.*, vol. 31, no. 7, pp. 603–632, Jul. 2006.
- [9] Y. Saito, J.-L. Putaux, T. Okano, F. Gaill, and H. Chanzy, "Structural Aspects of the Swelling of β Chitin in HCl and its Conversion into α Chitin," *Macromolecules*, vol. 30, no. 13, pp. 3867–3873, 1997.
- [10] H. K. No and S. P. Meyers, "Preparation and characterization of chitin and chitosan - A review.," *J. Aquat. Food Prod. Technol.*, vol. 4, no. 2, pp. 27–52, 1995.
- [11] K. Kofuji, Y. Huang, K. Tsubaki, F. Kokido, K. Nishikawa, T. Isobe, and Y. Murata, "Preparation and evaluation of a novel wound dressing sheet comprised of β -glucan–chitosan complex," *React. Funct. Polym.*, vol. 70, no. 10, pp. 784–789, Oct. 2010.
- [12] R. Tada, A. Tanioka, H. Iwasawa, K. Hatashima, Y. Shoji, K. I. Ishibashi, Y. Adachi, M. Yamazaki, K. Tsubaki, and N. Ohno, "Structural characterisation and biological activities of a unique type β -D-glucan obtained from *Aureobasidium pullulans*," *Glycoconj. J.*, vol. 25, no. 9, pp. 851–861, 2008.
- [13] G. D. Ross, V. Vetvicka, J. Yan, Y. Xia, and J. Vetvicková, "Therapeutic intervention with complement and beta-glucan in cancer.," *Immunopharmacology*, vol. 42, no. 1–3, pp. 61–74, 1999.
- [14] Y. Kimura, M. Sumiyoshi, T. Suzuki, and M. Sakanaka, "Antitumor and antimetastatic activity of a novel water-soluble low molecular weight beta-1,3-D-glucan (branch beta-1,6) isolated from *Aureobasidium pullulans* 1A1 strain black yeast," *Anticancer Res.*, vol. 26, no. 6B, pp. 4131–4141, 2006.
- [15] S. Gautier, E. Xhaufaire-Uhoda, P. Gonry, and G. E. Piérard, "Chitin-glucan, a natural cell scaffold for skin moisturization and rejuvenation," *Int. J. Cosmet. Sci.*, vol. 30, no. 6, pp. 459–469, 2008.
- [16] EFSA Panel on Dietetic Products Nutrition and Allergies (NDA), "Scientific Opinion on the safety of ' Chitin - glucan ' as a Novel Food," *EFSA J.*, vol. 8, no. 7, pp. 1–17, 2010.
- [17] J. L. Cereghino and J. M. Cregg, "Heterologous protein expression in the methylotrophic yeast

- Pichia pastoris*,” *Microbiol. Rev.*, vol. 24, pp. 45–66, 2000.
- [18] C. Roca, B. Chagas, I. Farinha, F. Freitas, L. Mafra, F. Aguiar, R. Oliveira, and M. A. M. Reis, “Production of yeast chitin – glucan complex from biodiesel industry byproduct,” vol. 47, pp. 1670–1675, 2012.
 - [19] S. R. Jameela and A. Jayakrishnan, “Glutaraldehyde cross-linked chitosan microspheres as a long acting biodegradable drug delivery vehicle: Studies on the in vitro release of mitoxantrone and in vivo degradation of microspheres in rat muscle,” *Biomaterials*, vol. 16, no. 10, pp. 769–775, 1995.
 - [20] E. Khor and L. Y. Lim, “Implantable applications of chitin and chitosan,” *Biomaterials*, vol. 24, no. 13, pp. 2339–2349, 2003.
 - [21] I. Farinha, P. Duarte, A. Pimentel, E. Plotnikova, B. Chagas, L. Mafra, C. Grandfils, F. Freitas, E. Fortunato, and M. A. M. Reis, “Chitin-glucan complex production by *Komagataella pastoris*: Downstream optimization and product characterization,” *Carbohydr. Polym.*, vol. 130, pp. 455–64, 2015.
 - [22] P. R. Austin, “Solvents for and Purification of Chitin,” *United States Pat.*, pp. 2–4, 1973.
 - [23] R. C. Capozza, “Solution of Poly(N-Acetyl-D-Glucosamine),” *United States Pat.*, pp. 1–8, 1975.
 - [24] C. Chiappe and D. Pieraccini, “Ionic liquids: Solvent properties and organic reactivity,” *J. Phys. Org. Chem.*, vol. 18, no. 4, pp. 275–297, 2005.
 - [25] T. P. Thuy Pham, C. W. Cho, and Y. S. Yun, “Environmental fate and toxicity of ionic liquids: A review,” *Water Res.*, vol. 44, no. 2, pp. 352–372, 2010.
 - [26] J. Ranke, K. Molter, F. Stock, U. Bottin-Weber, J. Poczbütt, J. Hoffmann, B. Ondruschka, J. Filser, and B. Jastorff, “Biological effects of imidazolium ionic liquids with varying chain lengths in acute *Vibrio fischeri* and WST-1 cell viability assays,” *Ecotoxicol. Environ. Saf.*, vol. 58, no. 3, pp. 396–404, 2004.
 - [27] S. Stolte, J. Arning, U. Bottin-Weber, M. Matzke, F. Stock, K. Thiele, M. Uerdingen, U. Welz-Biermann, B. Jastorff, and J. Ranke, “Anion effects on the cytotoxicity of ionic liquids,” *Green Chem.*, vol. 8, no. 7, pp. 621–629, 2006.
 - [28] D. Tao, Z. Cheng, F. Chen, Z. Li, N. Hu, and X. Chen, “Synthesis and Thermophysical Properties of Biocompatible Cholinium-Based Amino Acid Ionic Liquids,” *J. Chem. Eng. Data*, vol. 58, pp. 1542–1548, 2013.
 - [29] M. Petkovic, J. L. Ferguson, H. Q. N. Gunaratne, R. Ferreira, M. C. Leitão, K. R. Seddon, L. P. N. Rebelo, and C. S. Pereira, “Novel biocompatible cholinium-based ionic liquids—toxicity and biodegradability,” *Green Chem.*, vol. 12, no. 4, p. 643, 2010.
 - [30] R. A. Mantz, D. M. Fox, J. M. Green, P. A. Fylstra, H. C. De Long, and P. C. Trulove, “Dissolution of biopolymers using ionic liquids,” *Zeitschrift fur Naturforsch. - Sect. A J. Phys. Sci.*, vol. 62, no. 5–6, pp. 275–280, 2007.
 - [31] X. Yang, C. Qiao, Y. Li, and T. Li, “Dissolution and resourcefulization of biopolymers in ionic liquids,” *React. Funct. Polym.*, vol. 100, pp. 181–190, 2016.
 - [32] P. Bruin, M. F. Jonkman, H. J. Meijer, and a J. Pennings, “A new porous polyetherurethane wound covering,” *J. Biomed. Mater. Res.*, vol. 24, no. 2, pp. 217–226, 1990.
 - [33] K. Matsuda, S. Suzuki, N. Isshiki, K. Yoshioka, R. Wada, S. H. Hyon, and Y. Ikada, “Evaluation of a bilayer artificial skin capable of sustained release of an antibiotic,” *Biomaterials*, vol. 13, no. 2, pp. 119–122, 1992.
 - [34] J. A. Hirsch, S. A. Reddy, W. E. Capasso, and I. Linfante, “Non-invasive hemostatic closure devices: ‘Patches and pads,’” *Tech. Vasc. Interv. Radiol.*, vol. 6, no. 2, pp. 92–95, 2003.

- [35] Tegaderm product details. Available: http://www.3m.com/3M/en_US/company-us/all-3m-products/~/3M-Tegaderm-Pad-Film-Dressing-with-Non-Adherent-Pad?N=5002385+8707795+8707798+8710678+8710820+8711017+8711738+8717789+3293321914&rt=rud. Accessed 20/09/2016.
- [36] G. D. Mogoşanu and A. M. Grumezescu, "Natural and synthetic polymers for wounds and burns dressing," *Int. J. Pharm.*, vol. 463, no. 2, pp. 127–136, 2014.
- [37] R. Ardiyanti, "Design and Characterization of Chitin- Glucan Polymeric Structures for Wound Dressing Materials," no. Master Thesis, p. <https://run.unl.pt/handle/10362/13306>, 2014.
- [38] L. Greenspan, "Humidity fixed points of binary saturated aqueous solutions," *J. Res. Natl. Bur. Stand. Sect. A Phys. Chem.*, vol. 81A, no. 1, p. 89, 1977.
- [39] L. A. Neves, C. Afonso, I. M. Coelho, and J. G. Crespo, "Integrated CO₂ capture and enzymatic bioconversion in supported ionic liquid membranes," vol. 97, pp. 34–41, 2012.
- [40] A. Shefy-Peleg, M. Foox, B. Cohen, and M. Zilberman, "Novel Antibiotic-Eluting Gelatin-Alginate Soft Tissue Adhesives for Various Wound Closing Applications," *Int. J. Polym. Mater. Polym. Biomater.*, vol. 63, no. 14, pp. 699–707, 2014.
- [41] N. Muhammad, M. I. Hossain, Z. Man, M. El-Harbawi, M. A. Bustam, Y. A. Noaman, N. B. Mohamed Alitheen, M. K. Ng, G. Hefter, and C. Y. Yin, "Synthesis and physical properties of choline carboxylate ionic liquids," *J. Chem. Eng. Data*, vol. 57, no. 8, pp. 2191–2196, 2012.
- [42] J. Jacquemin, P. Husson, A. A. H. Padua, and V. Majer, "Density and viscosity of several pure and water-saturated ionic liquids," *Green Chem.*, vol. 8, no. 2, p. 172, 2006.
- [43] G. Quijano, A. Couvert, and A. Amrane, "Ionic liquids: Applications and future trends in bioreactor technology," *Bioresour. Technol.*, vol. 101, no. 23, pp. 8923–8930, 2010.
- [44] M. Bonhôte, P. Dias, A. Papageorgiou, N. Kalyanasundaram, K. and Gratzel, "Hydrophobic, Highly Conductive Ambient- Temperature Molten Salts," *Inorg. Chem.*, vol. 35, no. 12, pp. 1168–1178, 1996.
- [45] S. R. Cândido, "Design and Characterization of Novel Biopolymeric Structures using Biocompatible Ionic Liquids (MSc dissertation)," no. Master Thesis, p. <https://run.unl.pt/handle/10362/15748>, 2015.
- [46] D. J. S. Patinha, L. C. Tomé, H. Garcia, R. Ferreira, C. S. Pereira, L. P. N. Rebelo, and I. M. Marrucho, "The role of water in cholinium carboxylate ionic liquid's aqueous solutions," *J. Chem. Thermodyn.*, vol. 84, pp. 93–100, 2015.
- [47] H. V. Pawar, J. Tetteh, and J. S. Boateng, "Preparation, optimisation and characterisation of novel wound healing film dressings loaded with streptomycin and diclofenac," *Colloids Surfaces B Biointerfaces*, vol. 102, pp. 102–110, 2013.
- [48] D. Archana, J. Dutta, and P. K. Dutta, "Evaluation of chitosan nano dressing for wound healing : Characterization , in vitro and in vivo studies," *Int. J. Biol. Macromol.*, vol. 57, pp. 193–203, 2013.
- [49] T. Samanta, S. Sinha, and M. Mukherjee, "Effect of added salt on swelling dynamics of ultrathin films of strong polyelectrolytes," *Polymer (Guildf.)*, vol. 97, pp. 285–294, 2016.
- [50] B. D. Freeman, "Basis of Permeability/Selectivity Tradeoff Relations in Polymeric Gas Separation Membranes," *Macromolecules*, vol. 32, no. 2, pp. 375–380, 1999.
- [51] J. Wu and Q. Yuan, "Gas permeability of a novel cellulose membrane," vol. 204, no. January, pp. 185–194, 2002.
- [52] L. Liu, A. Chakma, and X. Feng, "Gas permeation through water-swollen hydrogel membranes," *J. Memb. Sci.*, vol. 310, no. 1–2, pp. 66–75, 2008.
- [53] M. S. Rao, S. R. Kanatt, S. P. Chawla, and A. Sharma, "Chitosan and guar gum composite

- films: Preparation, physical, mechanical and antimicrobial properties,” *Carbohydr. Polym.*, vol. 82, no. 4, pp. 1243–1247, 2010.
- [54] A. D. Sezer and E. Cevher, “Biopolymers as Wound Healing Materials: Challenges and New Strategies,” *Biomater. Appl. Nanomedicine*, pp. 383–414, 1992.
 - [55] L. Fan, H. Yang, J. Yang, M. Peng, and J. Hu, “Preparation and characterization of chitosan/gelatin/PVA hydrogel for wound dressings,” *Carbohydr. Polym.*, vol. 146, pp. 427–434, 2016.
 - [56] a Chenite, M. Buschmann, D. Wang, C. Chaput, and N. Kandani, “Rheological characterisation of thermogelling chitosan / glycerol-phosphate solutions,” *Carbohydr. Polym.*, vol. 46, pp. 39–47, 2001.
 - [57] J. Wu, J. Liu, Y. Shi, and Y. Wan, “Rheological, mechanical and degradable properties of injectable chitosan/silk fibroin/hydroxyapatite/glycerophosphate hydrogels,” *J. Mech. Behav. Biomed. Mater.*, vol. 64, pp. 161–172, 2016.

7. Appendices

Appendix I – Sugars calibration curves

Calibration for Glucose

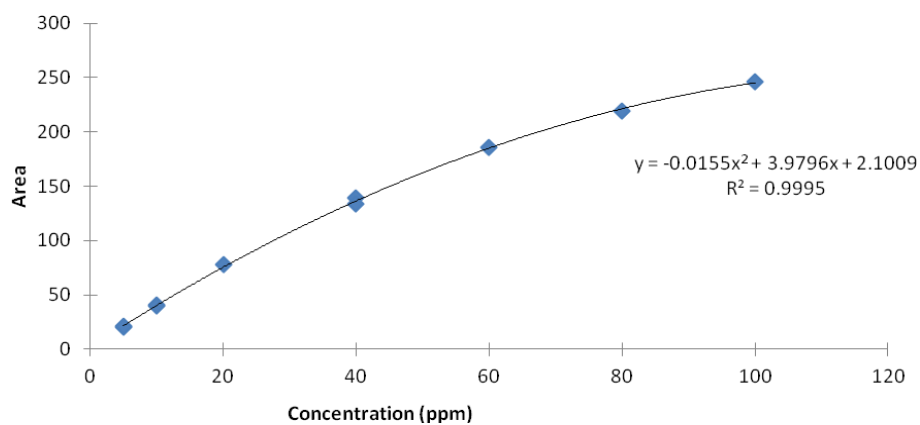


Figure 7.1 – Glucose calibration curve.

Calibration for Mannose

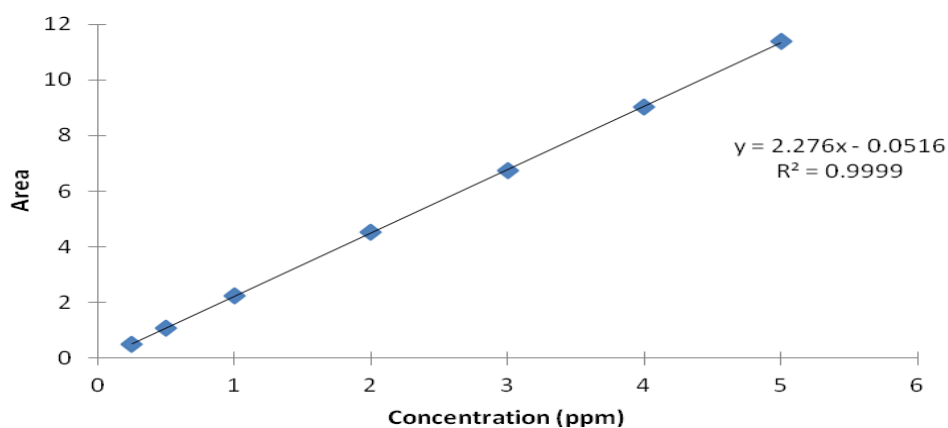


Figure 7.2 - Mannose calibration curves.

Calibration for Glucosamine

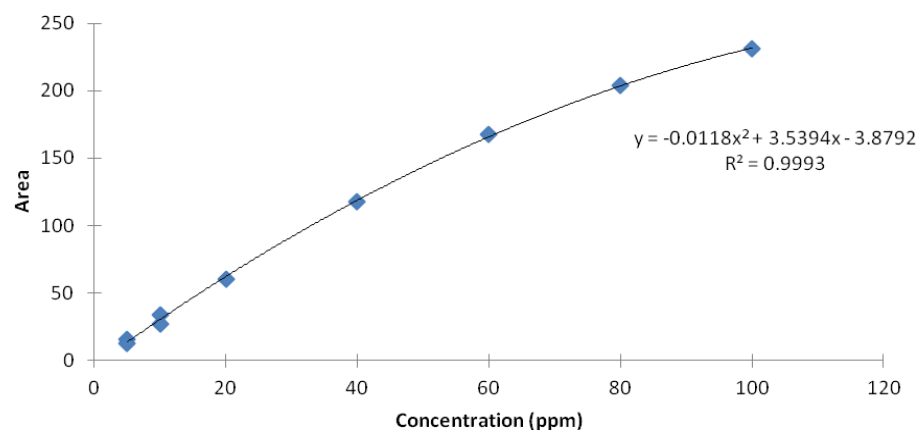


Figure 7.3 - Glucosamine calibration curve.

Appendix II – Flow curves for the different ionic liquids used

Choline Acetate

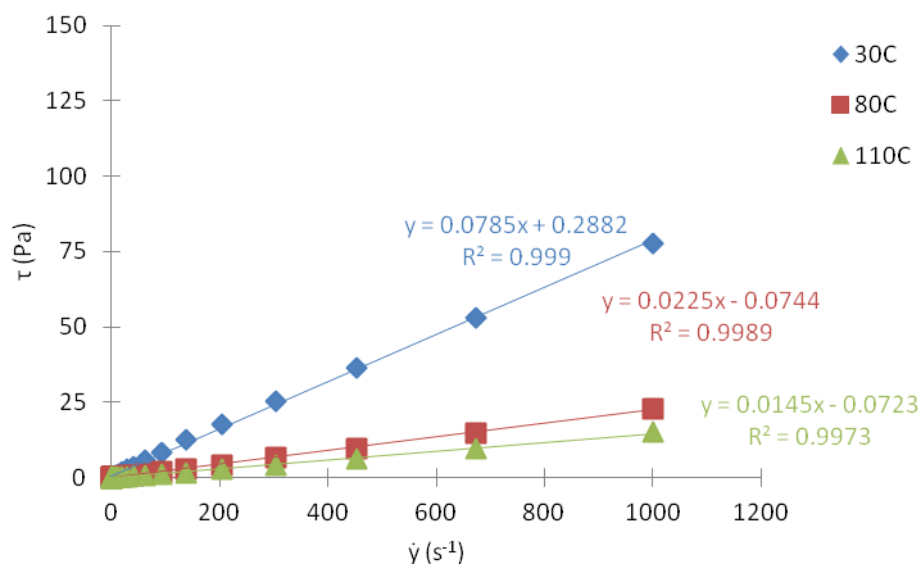


Figure 7.4 - Tension in function of the shear rate at different temperatures, 30°C, 80°C and 110°C, for choline acetate ionic liquid.

Choline Propionate

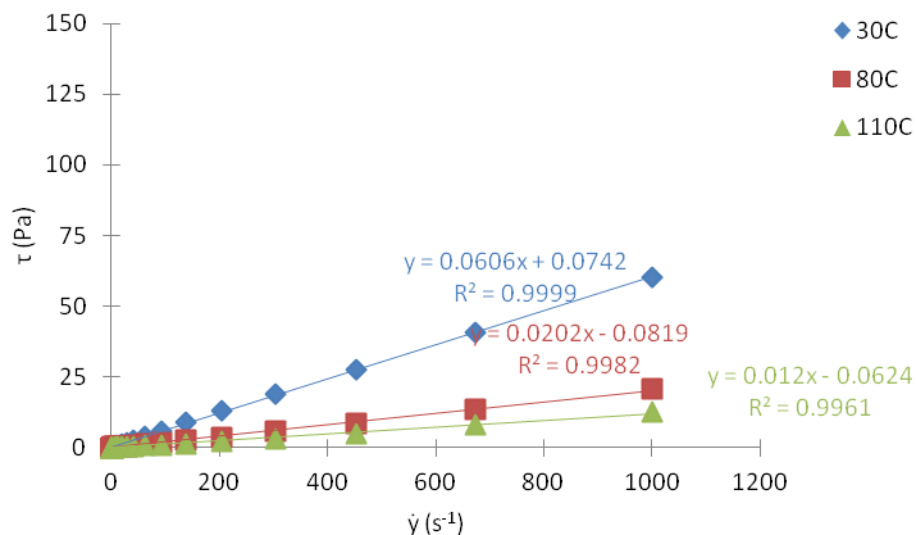


Figure 7.5 - Tension in function of the shear rate at different temperatures, 30°C, 80°C and 110°C, for choline propionate ionic liquid.

Choline Isobutanoate

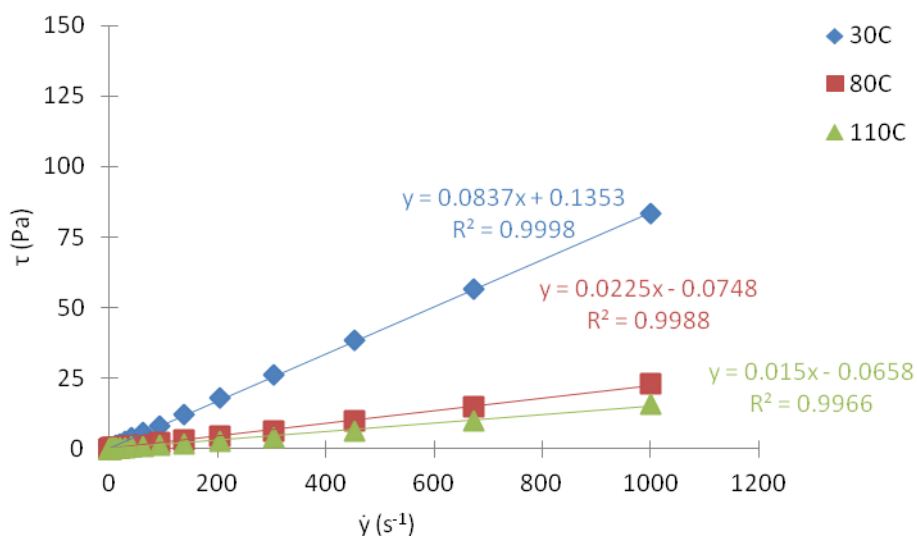


Figure 7.6 - Tension in function of the shear rate at different temperatures, 30°C, 80°C and 110°C, for choline isobutanoate ionic liquid.

Choline Hexanoate

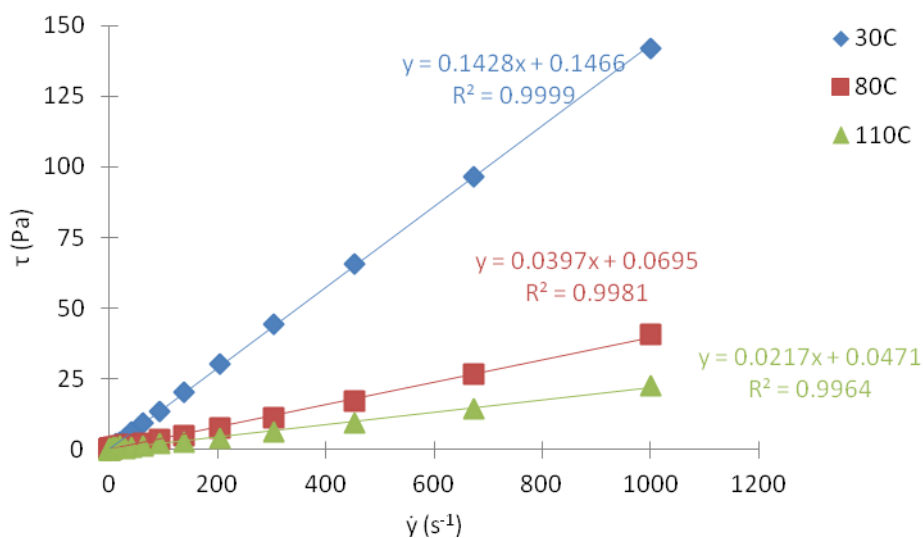


Figure 7.7 - Tension in function of the shear rate at different temperatures, 30°C, 80°C and 110°C, for choline hexanoate ionic liquid.

Appendix III – Linear representation of the activation energy

Choline Acetate

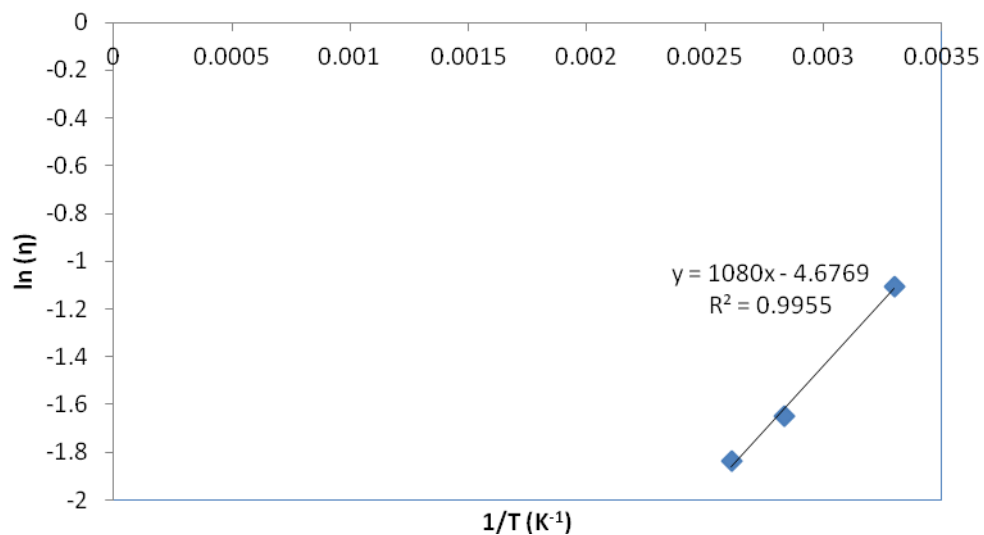


Figure 7.8 - Representation choline acetate viscosity as a function of temperature.

Choline Propionate

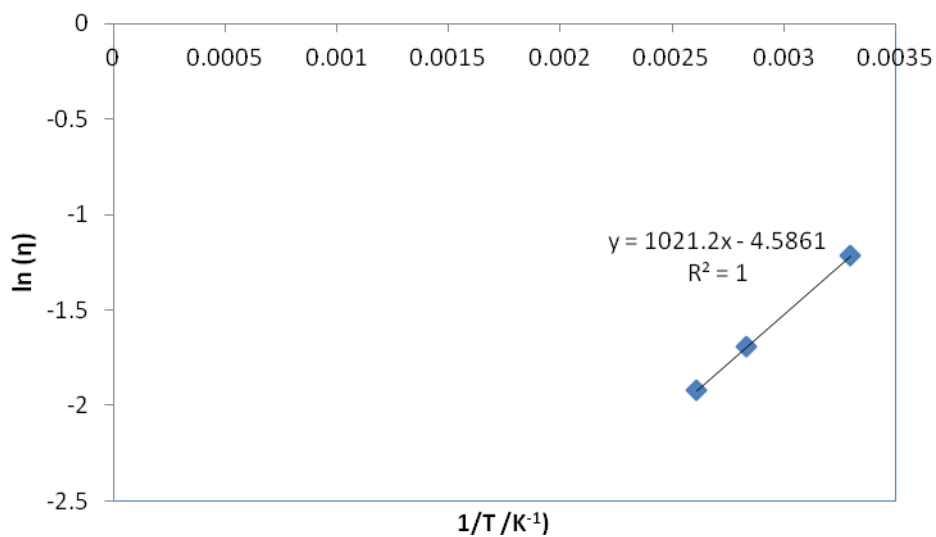


Figure 7.9 - Representation choline propionate viscosity as a function of temperature.

Choline Isobutanoate

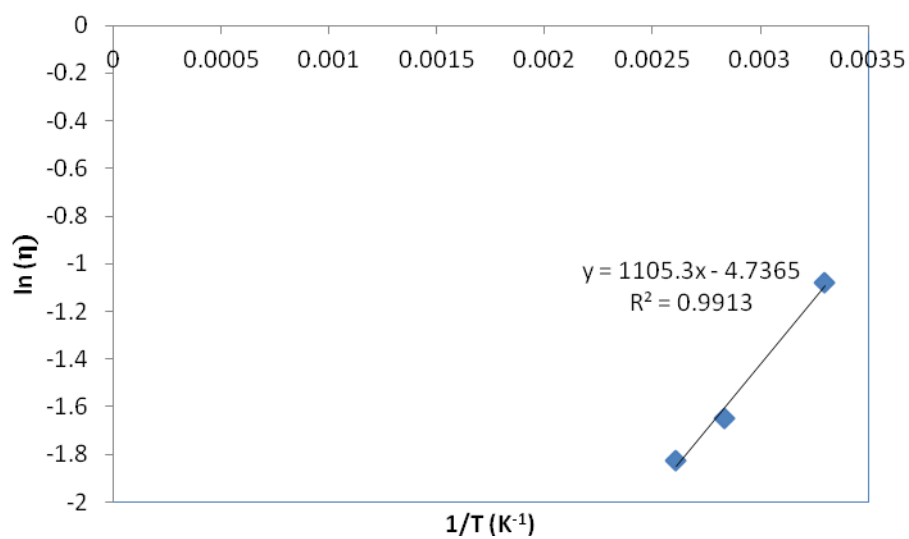


Figure 7.10 - Representation choline isobutanoate viscosity as a function of temperature.

Choline Hexanoate

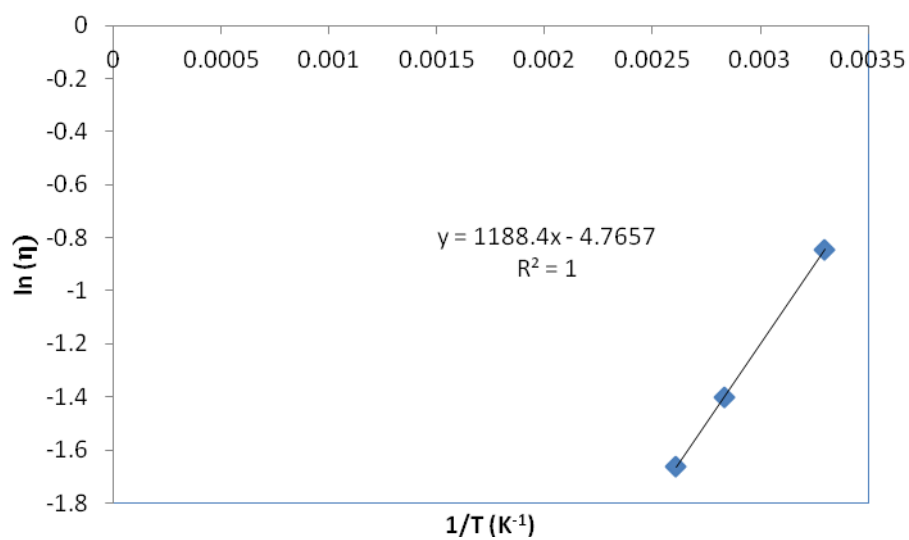


Figure 7.11 - Representation choline hexanoate viscosity as a function of temperature.

Appendix IV – Deformation curves of CGC-Com films

CAC

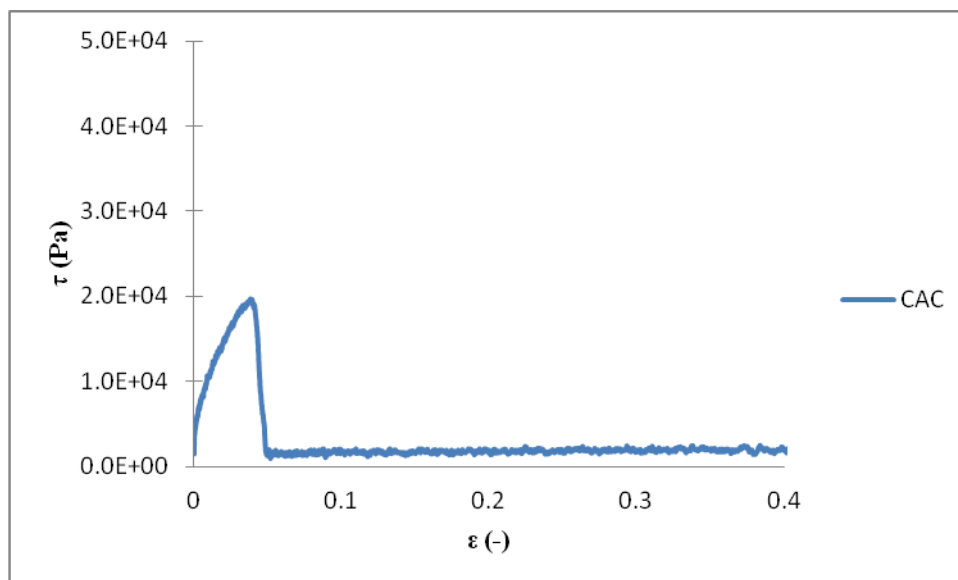


Figure 7.12 - Deformation curves of choline acetate CGC-Com.

CPC

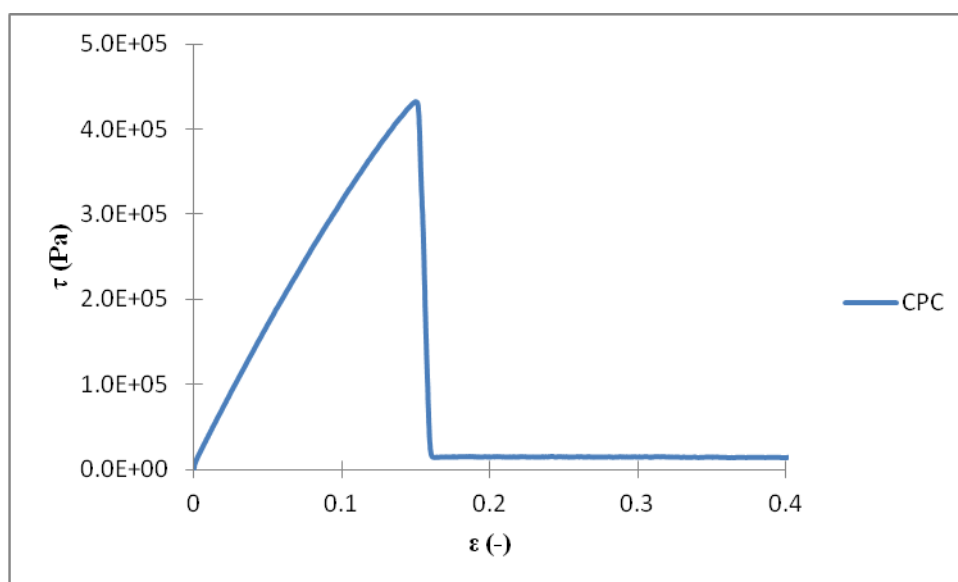


Figure 7.13 - Deformation curve of choline propionate CGC-Com.

CIC

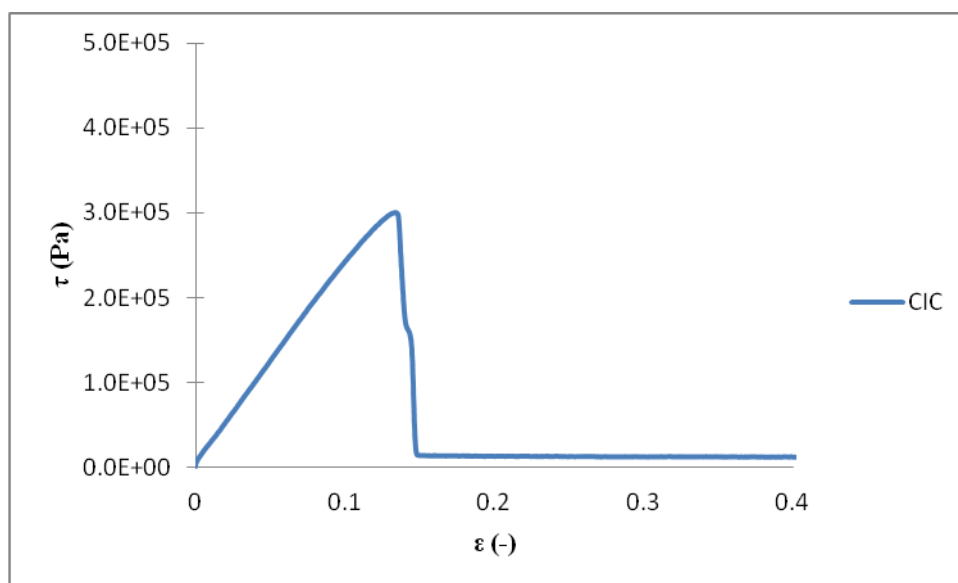


Figure 7.14 - Deformation curves of choline isobutanoate CGC-Com.

CHC

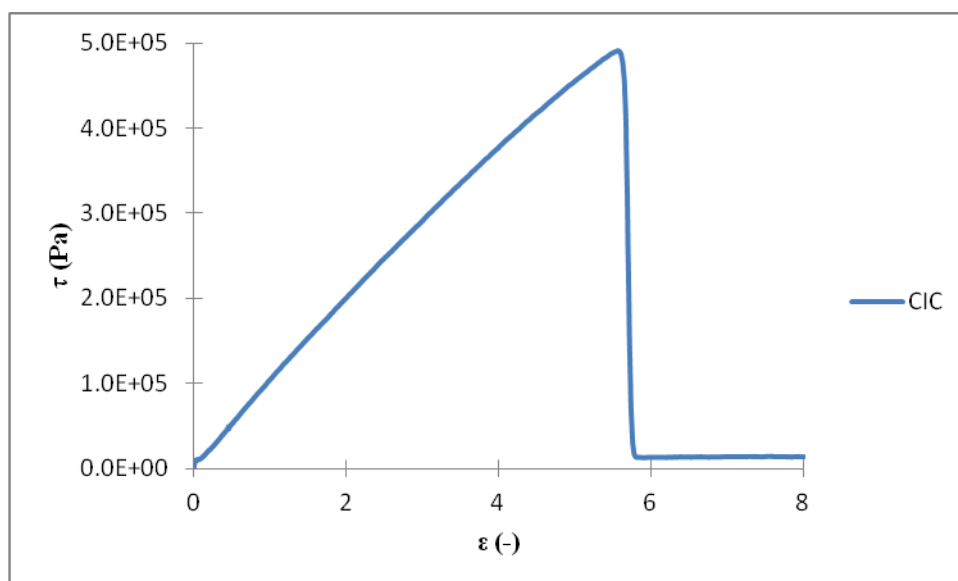


Figure 7.15 - Deformation curves of choline hexanoate CGC-Com.